Parameter calibration in a model of the secondary settling tank in wastewater treatment

Erik Lindahl

Master's thesis
2013:E36

Lund University

Faculty of Engineering
Centre for Mathematical Sciences
Mathematics

Centrum Scientiarum Mathematicarum

Parameter calibration in a model of the secondary settling tank in wastewater treatment

Erik Lindahl
Lund Institute of Technology

June 5, 2013

Abstract

In a wastewater treatment plant, particles (activated sludge) are separated from the liquid in a process called *continuous sedimentation*. This process is of crucial importance when purifying water in a wastewater treatment plant. This report will focus on a special case of sedimentation, namely *batch sedimentation*, which means that no flux into or out from the sedimentation tank are present. The goal is to implement and calibrate a mathematical model, that describes the phenomenon. During batch sedimentation, both in reality and in the model world, the conservation law implies solutions with *shock waves*. These shock waves set high standard for the numerical method used in the implementation. A specific model for this purpose is going to be used [3]. Some interesting results were found about the induction period in the initial phase of the sedimentation. Further improvements were observed when dispersion was taken into account in the model. Nevertheless, there is no doubt about the fact that more research in this area is needed.

Populärvetenskaplig sammanfattning

I ett vattenreningsverk separeras partiklar från en vätska under inflytande av gravitationen. Detta leder till en rening av avfallsvattnet. Det är av största vikt att matematiskt kunna beskriva denna process för att göra det möjligt att optimera driften i vattenreningsverken. Vattenrening är komplext och omfattar många olika vetenskapliga discipliner, såsom biologi, kemi, fysik och matematik. Denna masteruppsats kommer att behandla den fysikaliska och matematiska aspekten av processen. I den biologiska reningen i ett vattenreningsverk används sedimentering för att separera biologiskt slam från vattnet. Detta kallas kontinuerlig sedimentering, varvid två tankar är sammankopplade med varandra. Den ena består av ett substrat av aktiverat slam (mikroorganismer som förbrukar organiskt material). Denna benämns den biologiska reaktorn. I den andra tanken sker sedimenteringen. Sedimenteringstanken har ett inlopp och två utlopp. Inloppet består av aktiverat slam från den biologiska reaktorn. I toppen av tanken plockas sedan rent vatten ut, medan i botten det sedimenterade slammet återförs till den biologiska reaktorn. Systemet blir härvid återkopplat. Processen där inga flöden är kopplade till sedimenteringstanken kallas batchsedimentering, vilken denna masteruppsats har för syfta att undersöka.

Det har visat sig vara svårt att matematiskt kunna beskriva batchsedimentering. Till hands för analysen finns data från sedimenteringstest utförda av ett forskarlag i Belgien. Totalt tre experiment med olika initialkoncentrationer finns tillgängliga. Problemet är av sådan natur att partiella differentialekvationer, vars lösningar innehåller diskontinuiteter, så kallade chockvågor, uppkommer. Dessa ekvationer ställer höga krav på de numeriska algoritmer som används för att implementera lösarna och bara i undantagsfall går dessa ekvationer att lösa analytiskt.

För att till fullo kunna beskriva sedimentering av aktiverat slam måste kompression beaktas. Det betyder att när koncentrationen av partiklar överskrider en viss kritisk koncentration börjar partiklarna att röra vid varandra och en kompressionseffekt uppstår. Det är inte känt vid vilken koncentration detta sker eller hur stor effekten är.

Resultaten från analysen visar att denna kritiska koncentration verkar vara svår att finna. De modeller som använts är konservationslagar samt vissa konstitutiva antaganden om partiklarnas sjunkegenskaper. Givet denna modell och tillgängliga data ger analysen inget entydigt svar om den kritiska koncentrationen. Ej heller hur stor effekten skulle vara. Emellertid visar det sig att induktionsperioden för höga initialkoncentrationer spelar en avgörande roll. Vidare har det visat sig att, trots beaktande av induktionsperioden, problemet är illa konditionerat. Slutsatsen är att mer forskning på området behövs för att lösa dessa problem.

Contents

1 Introduction

The aim of this master thesis is to provide a parameter calibration of a specific mathematical model describing a phenomenon called *batch sedimentation*. In a wastewater treatment plant, the activated sludge particles are separated from the liquid in a process called *activated sludge process*. This process can be described with two tanks connected to each other. One with the activated sludge, i.e. a tank where microorganisms consume and decompose organic material. This is called the *biological reactor*. In the other tank, called the *settler*, the particles will be separated from the liquid. In the settler, there are one inlet and two outlets. The inlet consists of activated sludge from the biological reactor. On the top of the settler purified water is obtained and in the bottom waste sludge leaves the settler. Some of the waste sludge is recycled, which means that it recirculates back to the biological reactor [4]. *Batch sedimentation* is the process when no out- or inlets are considered, i.e. the settler has a total flux of zero on the top and the bottom of the tank. This thesis will discuss some properties of batch sedimentation with a certain initial concentration. This, together with the boundary condition (total flux is zero on the top and the bottom if the tank) produces an initial-boundary-value problem, which we will discuss later in this paper.

When the concentration of sludge in the sedimentation tank exceeds a critical concentration, the particles start to touch each other and therefore transmit solid stress. This will lead to *compression* of the particles. It is unknown how this effective solid stress function looks like. The main topic of this thesis is to find an appropriate model structure and calibrate its parameters. Earlier attempts to solve this problem have shown that the problem is ill-posed i.e. the solutions are not unique [2].

In 2005 data from a Wastewater treatment plant in Deinze, Belgium, were collected by a research team [1]. Totally three sets of data are available in the analysis, with three different initial concentrations of the activated sludge. With help from this data, we hope to find a model that fully can describe batch sedimentation in mathematical terms. The idea is then to use this new knowledge in the continuous sedimentation case.

To get an introduction for the mathematical model that describes the phenomena above, Section 2 will briefly discuss the *traffic flow problem* [9], which can be described by the same differential equations as batch sedimentation. In Section 3 we will go back to sedimentation again. In Section 4 we will take a look at the numerical implementation of the batch sedimentation PDE and test the solver for some simple cases. Section 5 treats a minimization problem, where the goal is to find parameter values for the model, by fit the model to synthetic data and in Section 6 this is repeated, but now with real data collected by [2]. In Section 7 and 8 the approach is different from that in Section 6, but with the same goal; to find parameter values, i.e calibrate the model, by using the measured data. Section 9 discusses the results and some improvements to the model are also suggested.

2 Introductory example

Here we will consider the traffic flow problem, by assuming the road to be in one dimension, say x direction. Denote the concentration of cars along the road by u. Then u is a function of x and time t, $u = u(x,t)$. By using the principle of conservation, the rate of change of the total number of cars on the road is equal to the inward flux of cars minus the outward flux of cars. This function, f, is also a function of x and t, $f = f(x,t)$. Now, consider an x interval (x_0, x_1). The conservation law can then be written in the following way [6]:

$$\frac{d}{dt}\int_{x_0}^{x_1} u(x,t)dx = f(x_0,t) - f(x_1,t) \tag{1}$$

where $f(x_0,t)$ is the flux of cars into the road and $f(x_1,t)$ is the flux of cars out from the road. Equation (1) can, by taking the derivative inside the integral sign, be formulated as

$$\int_{x_0}^{x_1} \frac{\partial u}{\partial t}dx \tag{2}$$

By the same technique the right hand side of (1) can be written as

$$-\int_{x_0}^{x_1} \frac{\partial f}{\partial x}dx \tag{3}$$

Putting together (1),(2) and (3) it must hold that

$$\int_{x_0}^{x_1} \left(\frac{\partial u}{\partial t} + \frac{\partial f}{\partial x}\right) dx = 0. \tag{4}$$

We can take *any* interval (x_0, x_1) which implies that

$$\frac{\partial u}{\partial t} + \frac{\partial f}{\partial x} = 0. \tag{5}$$

This is a partial differential equation. If the function f only depends on u, $f = f(u(x,t))$, (5) will be a partial differential equation for u in the variables x and t. From now on we assume that f only depends on $u(x,t)$. To get a reasonable realistic model for the flux, we have to take into account the speed of the cars, v, as a function of the concentration u. Here we assume that the speed is v_0 when $u = 0$ and $v = 0$ when $u = u_{\max}$. Between these two extremes we assume that the speed decreases linearly, making v to look like [9]

$$v = v(u) = v_0\left(1 - \frac{u}{u_{\max}}\right) \tag{6}$$

The flux can then be obtained as the concentration multiplied by the speed, in mathematical terms:

$$f = f(u) = v(u)u = uv_0\left(1 - \frac{u}{u_{\max}}\right) \tag{7}$$

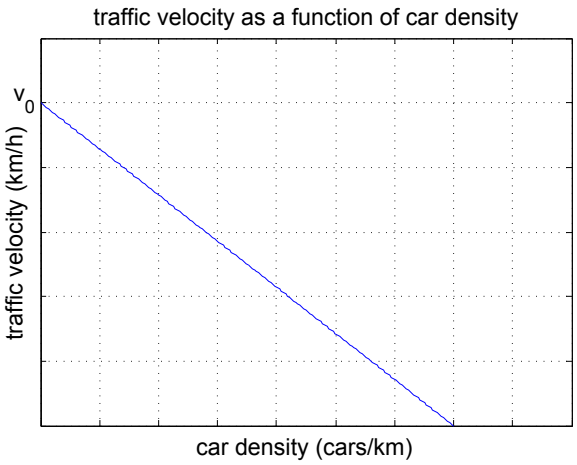

Figure 1: Velocity as a function of traffic density.

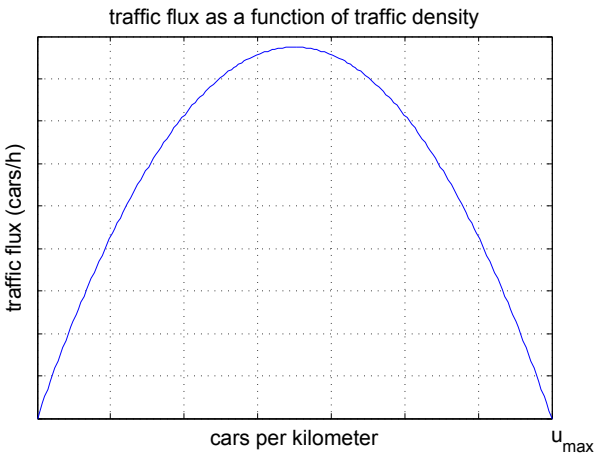

Figure 2: Flux as a function of traffic density.

Here the function f has a second degree dependence of u and the derivative of f with respect to u is a decreasing function of u. Combination of Equation (5) and (7) gives the equation (by taking the derivative of f with respect to x and u with respect to t) [6]

$$u_t + f'(u)u_x = 0. \tag{8}$$

Clearly, (7) is not linear because the coefficient for u_x depends on u itself. To solve a partial differential equation like (8), an initial distribution has to be imposed. System (9) is the general form for this problem:

$$\begin{cases} u_t + f'(u)u_x = 0, & x \in \mathbb{R}, \quad t > 0 \\ u(x,0) = u_{\text{init}}(x), & x \in \mathbb{R} \end{cases} \tag{9}$$

where $u_{\text{init}}(x)$ is the concentration for $t = 0$. To solve a system like (9) it is a good idea to use the method of characteristics. Therefore, consider a curve $x(t)$ in the x-t-plane where u is constant, u_0, meaning that $x(t)$ is a *level curve* for u. Plug $x = x(t)$ into u and get:

$$u(x(t), t) = u_0. \tag{10}$$

Taking the derivative with respect to t using the chain rule:

$$u_x x'(t) + u_t = 0 \tag{11}$$

Now, replace u_t with $-f'(u)u_x$ according to Equation (8) and obtain

$$u_x(x'(t) - f'(u_0)) = 0 \tag{12}$$

From Equation (12) it follows that either $x'(t) = f'(u_0)$ or $u_x = 0$. If $u_x = 0$, Equation (8) implies $u_t = 0$, so the solution u is constant, u_0, along i straight line in the x-t-plane. If instead $x'(t) = f'(u_0)$ this also means that the solution is constant along i straight line. The slope of the level curves (which also are called characteristics) in the x-t-plane has the value $1/f'(u_0)$. Here we define the *signal speed* as the value $f'(u_0)$,

because a wave will propagate with this speed. From the relation $x'(t) = f'(u_0)$ it is easy to integrate over time and get $x(t) = f'(u_0(x_0))t + x_0$ for all points x_0 on the x axis. For $x = x_0$ we have $u = u_0(x_0)$ and this produces an implicit relation between u, x and t formulated in system (13): [6]

$$\begin{cases} x = f'(u_0(x_0))t + x_0 \\ u = u_0(x_0) \end{cases} \tag{13}$$

In some cases it is possible to achieve a solution u from system (13) explicitly, but this is not always the case. Another possibility is to construct solutions geometrically. The following example will show how to do this.

Example 1

The initial value problem

$$u_t + uu_x = 0 \tag{14}$$

with initial condition

$$u_0(x) = \begin{cases} 0, & x \leq 0 \\ x, & 0 \leq x \leq 1 \\ 1, & x \geq 1 \end{cases}$$

can be solved geometrically. From (14) we conclude that $f(u) = \frac{1}{2}u^2$ and since $f'(u) = u$ it follows that the signal speed is zero for $x \leq 0$, increases linearly in the range $0 \leq x \leq 1$ and is constant $= 1$ for $x \geq 1$. Figure 3 shows the characteristics starting from the different regions on the x-axis and Figure 4 shows $u(x, 0)$, $u(x, 1/2)$ and $u(x, 1)$. By using the system (13), or Figure 3, one can explicitly solve Equation

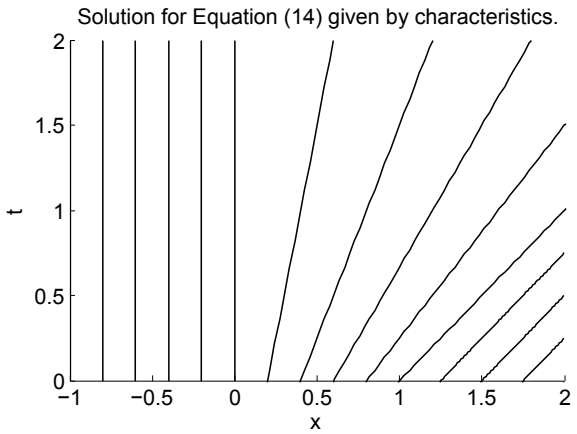

Figure 3: Solution for Equation (14) in terms of characteristics.

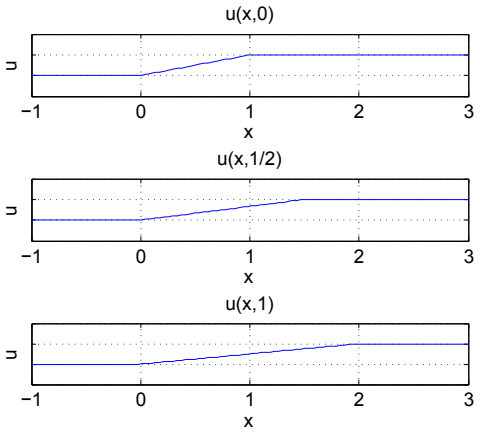

Figure 4: Solution for Equation (14) for $t = 0, 1/2, 1$.

(14) with the given initial condition. The solution reads

$$u(x,t) = \begin{cases} 0, & x \leq 0 \\ \frac{x}{1+t}, & 0 \leq x \leq 1+t \\ 1, & x \geq 1+t \end{cases}$$

One interesting question immediately arises; what happens if two characteristics intersects? The next example will partly answer this question.

Example 2

The equation is the same as in (14) but with different initial condition. The problem to be solved is

$$u_t + uu_x = 0 \tag{15}$$

$$u_0(x) = \begin{cases} 1, & x \leq 0 \\ 1 - x, & 0 \leq x \leq 1 \\ 0, & x \geq 1 \end{cases}$$

By using the same technique as in example 1, characteristics can be drawn from the x-axis over the $x - t$-plane. This is shown in Figure 5. What happens in the point

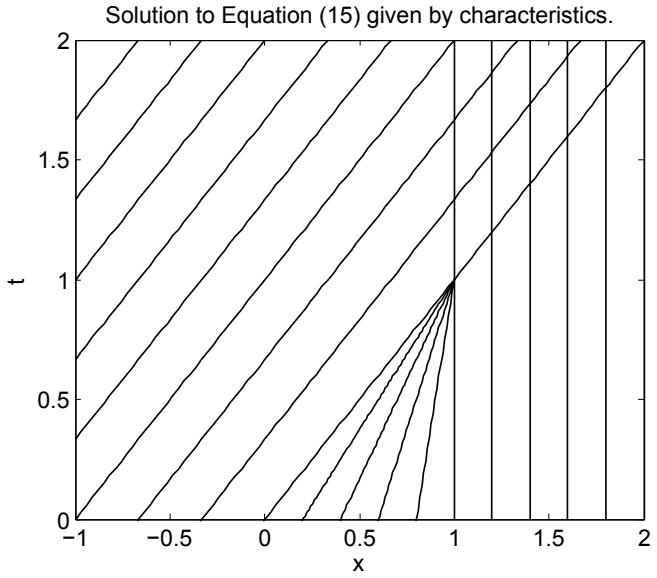

Figure 5: Solution for Equation (15) in terms of characteristics.

$(1, 1)$ is that several characteristics intersects. It is no longer possible to achieve a continuous solution, a *shock wave* is obtained. The next section will briefly discuss these properties.

2.1 Discontinuities and shock waves

This section will deal with what is happening when discontinuities appear. We are going to make use of the concept *weak solution*. If it is possible to express x_0 in terms of x and t in the first equation in system (13) and plug it into the second equation, a C^1-solution can be obtained. C^1 stands for continuously differentiable functions. It can be shown that a C^1-solution can be obtained precisely when

$$\frac{dx}{dx_0} = f''(u(x_0)u_0'(x_0)t + 1 \neq 0 \tag{16}$$

where the implicit function theorem has been used. From (16) we see that, for some functions f and the sign of $u_0'(x_0)$, there exists a time t for which

$$\frac{dx}{dx_0} = f''(u(x_0)u_0'(x_0)t + 1 = 0 \tag{17}$$

The smallest time t that satisfy (17) is called the *critical time.* Beyond this time, a weak formulation of the conservation law must be used in order to get a solution. Now, multiply Equation (8) with a function w that belongs to C_0^1, which stands for continuously differentiable function with compact support. Compact support means that the function is zero outside a compact interval. Now, use partial integration, and get the relation

$$\int_0^\infty \int_{-\infty}^\infty (uw_t + f(u)w_x)\, dx\, dy \; + \int_{-\infty}^\infty u(x,0)w(x,0)dx = 0 \tag{18}$$

This must hold for all $w \in C_0^1$. If a function u satisfies Equation (18) this function is a weak solution of Equation (8). It is now possible to deal with the discontinuities in order to get a solution. But the question still remains; what is happening at the discontinuity? Therefore, consider a curve $x(t)$ where the solution has a discontinuity. Assume $x(t) \in C^1$. Introduce an interval (a, b) which intersects the curve and is parallel to the x-axis and denote the solution u^- to the left of $x(t)$ and u^+ to the right of $x(t)$. Use Equation (1) for (a, b):

$$f(u(a,t)) - f(u(b,t)) = \frac{d}{dt}\int_a^b u dx = \frac{d}{dt}(\int_a^{x(t)} u dx + \int_{x(t)}^b u dx) \tag{19}$$

Now, take the derivation inside the integral sign (this is possible because $x(t)$ and u are sufficiently smooth). Hence (19) becomes

$$\int_a^{x(t)} u_t dx + u^- x'(t) + \int_{x(t)}^b u_t dx - u^+ x'(t). \tag{20}$$

From Equation (5), $u_t = -f_x$, so (19) and (20) combined then gives

$$f(u(a,t)) - f(u(b,t)) = f(u(a,t)) - f(u(b,t)) + f(u^+) - f(u^+) - (u^+ - u^-)x'(t) \tag{21}$$

Rearrange (21), then $x'(t)$, which is the speed of the discontinuity, can be expressed as

$$x'(t) = \frac{f(u^+) - f(u^-)}{u^+ - u^-} \tag{22}$$

Equation (22) is of central importance. It is called the *jump condition* or *Rankine-Hugoniot condition* after William John Macquorn Rankine and Pierre Henri Hugoniot. A weak solution of (18) is obtained if system (9) is satisfied in the domain where $u \in C^1$ and the jump condition is fulfilled where u has discontinuities. This is actually not enough to get the correct physical solution of system (9). An additional condition has to be imposed, namely the *Entropy Condition.* This condition will help

us to pick out the physical correct shock wave. The problem with weak solutions is that they are not unique. It can be shown that

$$f'(u^-) \geq x'(t) \geq f'(u^+) \tag{23}$$

must hold in order to get a unique solution to Equation (18). Condition (23) is the entropy condition and this, together with the jump condition and a convex or concave flux function, makes it possible to receive a solution.

3 Batch sedimentation

Batch sedimentation shares a lot of similarities with the traffic flow problem described in Chapter 2. The underlying physics is almost the same. There will appear solutions with shock waves. Consider a cylindrical tank with given height and radius. The tank is filled with a homogeneous suspension of particles and liquid. It can be assumed that no inward or outward flux are present. This is called *batch sedimentation*. The gravity will force the particles to the bottom of the tank, leaving the clear liquid at the upper most top of the tank. By using the conservation law described in Chapter 2, some assumtions about the flux present at the bottom and the top of the tank and some initial distribution, an initial-value-boundary-value problem arises. We also assume the problem to be in one spatial dimension, x-direction and time t. The x-axis points upwards and the tank has its top at $x = h$ and its bottom at $x = 0$. The flux function f and the velocity, here called v, are positive in the negative x-direction. Denote the concentration of the particles by u. Then u is a function of x and t, $u = u(x, t)$. As in Chapter 2, suppose the velocity of the particles, to depend only on the concentration, making $v = v(u)$. For a flux function with one inflection point and $u_0(x)$ as the initial distribution of the suspension the following initial-boundary-value problem is obtained [3], [8]:

$$\begin{cases} u_t - f(u)_x = 0, & 0 < x < h, \quad t > 0, \\ u(x, 0) = u_0(x), & 0 < x < h, \\ u(0^+, t) = u_{\max}, & t > 0, \\ u(h^-, t) = 0, & t > 0, \end{cases} \tag{24}$$

The last two equations in system (24) come from the fact that the flux is zero at the top and the bottom of the tank. The values of u for which the flux is zero are either $u = 0$ or $u = u_{\max}$. After the system is released the concentration will immediately reach $u = u_{\max}$ at the bottom of the tank and $u = 0$ at the top of the tank. It should also be observed the minus sign in the first equation due to the orientation of the x-axis. We will now discuss the solution of problem (24) for three different flux functions. They are plotted in Figures 6-9 respectively.

Case I

The flux function reads $f(u) = u(u_{\max} - u)$ where the function is scaled so that $u_{\max} = 1$. It follows that $f''(u) = -2$, so the necessary condition for an inflection point, namely that $f''(u) = 0$, can not be fulfilled. Now, suppose the initial distribution is u_0 homogeneously in the tank, where u_0 is somewhere between 0 and $u_{\max}$. Using the method of characteristics, we can solve this problem. For the problem of sedimentation it is more natural to have the t variable as the independent variable and the x variable as the dependent variable. By drawing the characteristics in the different regions in the t-x-plane and use the jump condition the solution can be constructed, see Figure 10. The bold lines shows two different shock waves. One is transported from the top to the bottom and one is transported from the bottom to the top. Clearly, after a certain finite time, t_{end}, the solution is stationary, where

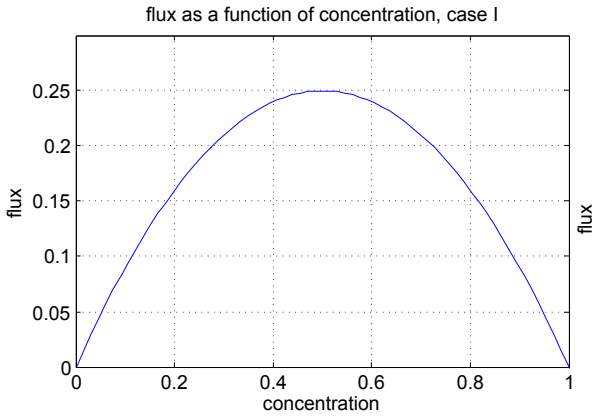

Figure 6: Flux as a function of concentration, case I.

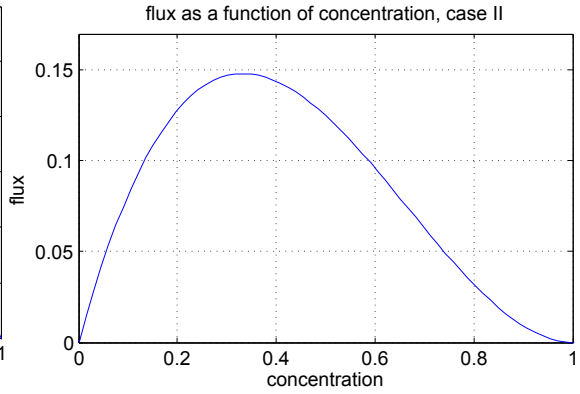

Figure 7: Flux as a function of concentration, case II.

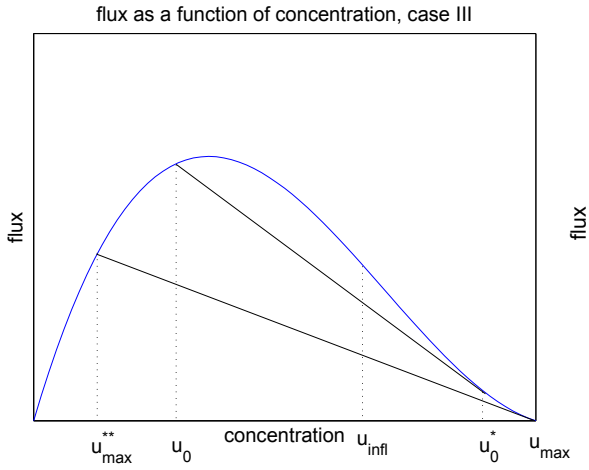

Figure 8: Flux as a function of concentration, case III(a).

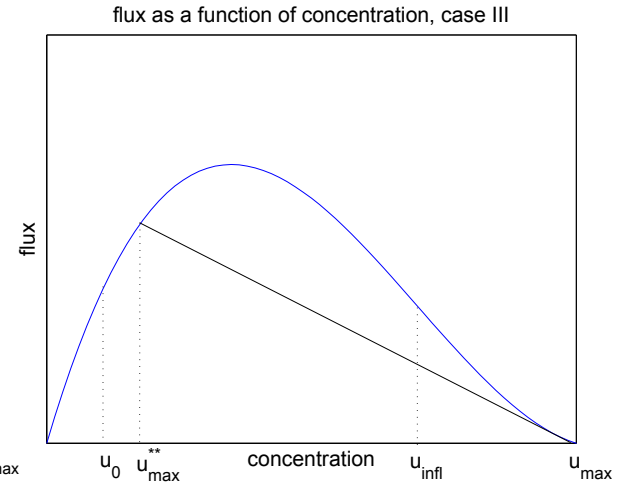

Figure 9: Flux as a function of concentration, case III(b).

the two shock waves meet. After this time, the shock speed is zero. This means that the concentration is $u = 0$ for $x < x_{\text{limit}}$, and $u = u_{\max}$ for $x > x_{\text{limit}}$. Here x_{limit} denotes the border between the clear liquid and the part of the tank where the concentration is homogeneously $u = u_{\max}$. By knowing the slope of the bold lines, i.e. the shock speed, one can calculate t_{end} and x_{limit}. The slope of the upper shock is $u_{\max} - u_0$ so the equation for this straight line is $x_1(t) = (u_{\max} - u_0)t + h$ and for the lower $x_2(t) = -u_0 t$. Put $x_1(t_{\text{end}}) = x_2(t_{\text{end}})$ and get $t_{\text{end}} = (h/u_{\max})$ and $x_{\text{limit}} = u_0(h/u_{\max})$.

Case II

Now the flux function is $f(u) = u(u - u_{\max})^2$, so $f'(u) = (u - u_{\max})^2 + 2u(u - u_{\max})$ and $f''(u) = 6u - 4u_{\max}$. It is clear that $f'(u_{\max}) = 0$ and $f''((2/3)u_{\max}) = 0$, meaning that f has an inflection point at $u = (2/3)u_{\max}$. The fact that $f'(u_{\max}) = 0$ and the inflection point located at $u = (2/3)u_{\max}$ makes the situation different from that in

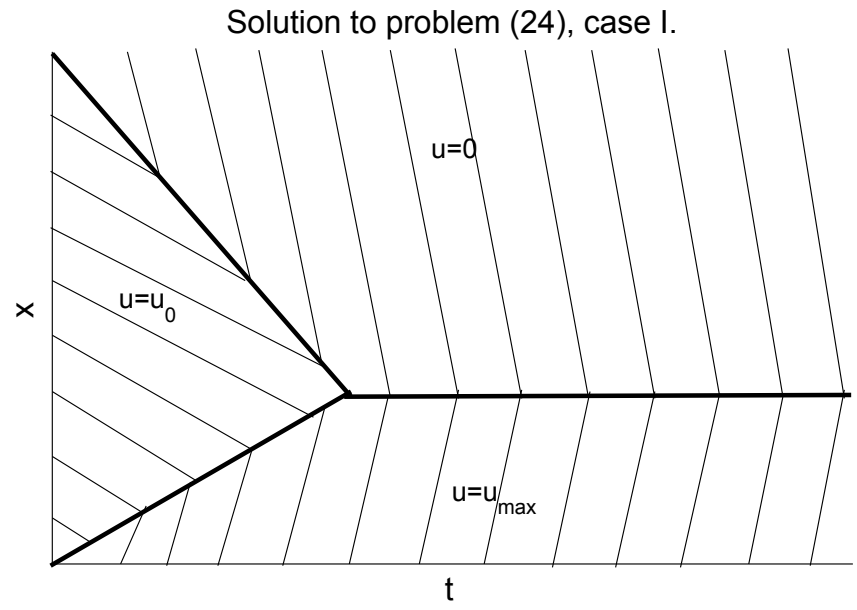

Figure 10: Solution to problem (24), case I.

case I. Figure 11 shows what is going on. The bold line at the right in the figure shows

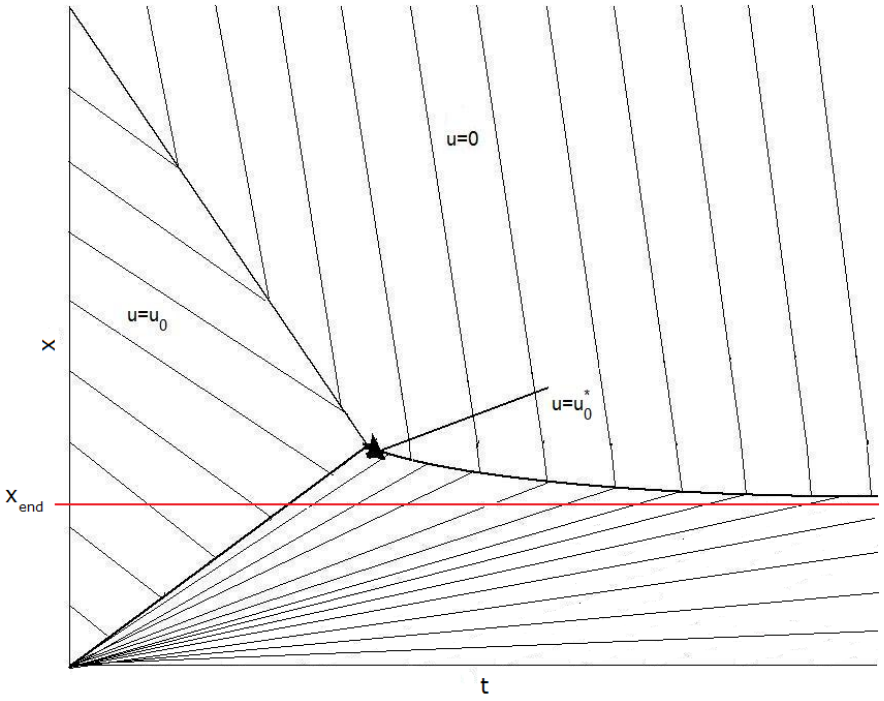

Figure 11: Solution to problem (24), case II.

a shock wave that has not constant speed. Below this line u will grow to $u = u_{\max}$ as $t \to \infty$. The system becomes asymptotically stationary. By using the fact that the total mass in the tank remains constant it must hold that $Ahu_0 = Ax_{\text{end}}u_{\max}$, where A is the cross-sectional area, and thus $x_{\text{end}} = hu_0/u_{\max}$.

Case III

The flux function here is $f(u) = u(u - 1.05)^2 - \varepsilon u$, where $\varepsilon = 0.0025$. We have defined $u_{\max} = 1$ so that $f(0) = f(u_{\max}) = 0$ and $f'(u_{\max}) = -\varepsilon$. Consider Figures 8 and 9. Here we have $f'(u_{\max}) > 0$. Two qualitatively different situations now occur, depending on the size of u_0. The first case **(b)** is when $u_0 < u^{**}_{\max}$, see Figure 9. This case is the same as in case I, because the inflection point does not affect the system. If instead $u_0 > u^{**}_{\max}$, (case **(a)**, as seen in Figure 8, the solution is found in Figure 12. The inflection point makes it impossible for a shock wave to travel from u_0 directly to $u_{\max}$. Instead an expansion wave will be observed from u^*_0 to $u_{\max}$. It should also be taken into consideration that in case II, $u^{**}_{\max} = 0$. With the same argument as in case II, $x_{\text{end}} = hu_0/u_{\max}$ and since we know the slope of the characteristic that passes through the point $(t_{\text{end}}, x_{\text{end}})$ we can calculate t_{end} as $t_{\text{end}} = (x_{\text{end}} - h)/f'(u_{\max})$. Note that $t_{\text{end}} \to \infty$ as $f'(u_{\max}) \to 0$.

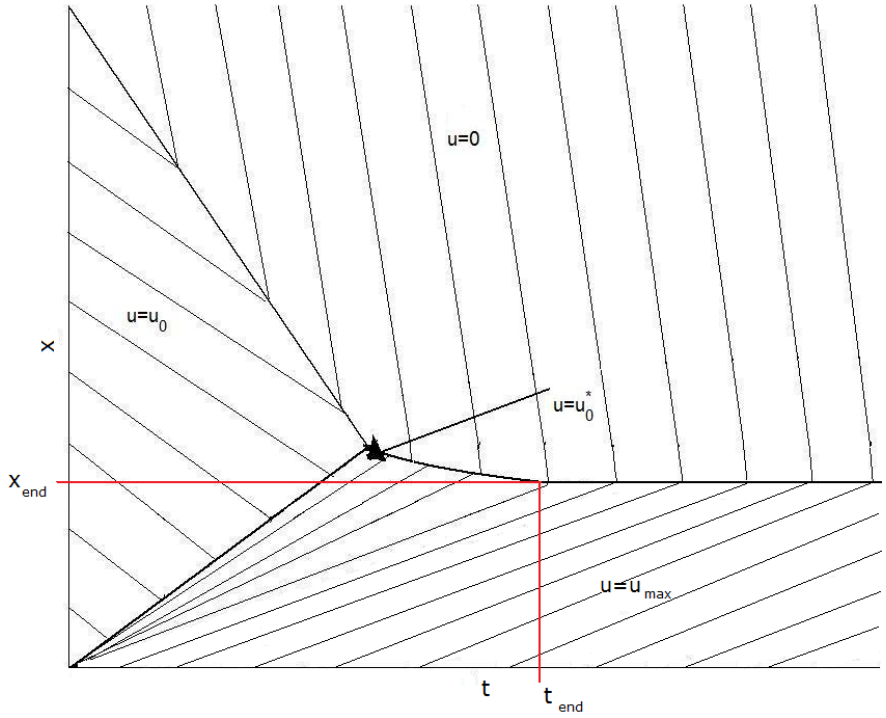

Figure 12: Solution to problem (24), case III(b).

4 Numerical method for batch sedimentation PDE

4.1 Models of batch and continuous sedimentation

In Chapter 3 some simple cases of batch sedimentation were treated. In this Chapter we will introduce a new physical phenomenon to the model, namely *compression.* When the concentration exceeds a critical concentration, u_c, the particles start to touch each other, which means that they will be exposed to solid stress. The constitutive relation that governs this solid stress is one of the main topic of this paper. The following model, for *continuous* sedimentation, is described by [3] and [4], see Figure 13 and 14:

$$\frac{\partial u}{\partial t} + \frac{\partial}{dx} F(u,x,t) = \frac{\partial}{dx}\left(\{\gamma(x) d_{\text{comp}}(u) + d_{\text{disp}}(x, Q_{\text{f}}(t))\} \frac{\partial u}{\partial x} \right) + \frac{Q_{\text{f}}(t) u_{\text{f}}(t)}{A} \delta(x) \tag{25}$$

Here u is the concentration, F is the convective flux, x the spatial variable (assuming

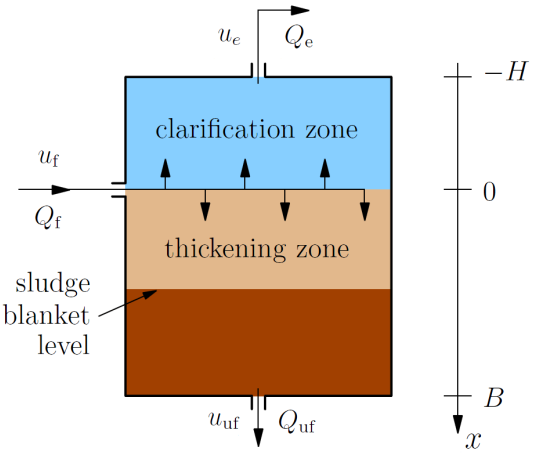

Figure 13: Continuous sedimentation.

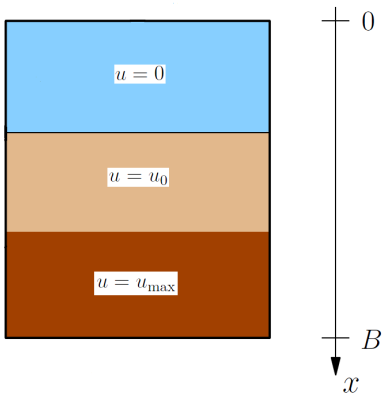

Figure 14: Batch sedimentation.

the problem to be in one space dimension), t time, $\gamma(x)$ a function that is 1 where compression is present and 0 otherwise, d_{comp} a function that models the compression due to solid stress, d_{disp} a function that models dispersion due to turbulence, $Q_{\text{f}}(t)$ the volumetric feed flow, u_{f} the feed concentration and $\delta(x)$ the Dirac delta distribution.

In the case of batch sedimentation, Equation (25) will be substantially simplified. We can suppose that no dispersion has to be considered, making $d_{\text{disp}} \equiv 0$ and also, $Q_f(t) \equiv 0$. Equation (25) is a result of the conservation law described in Chapter 2. In our case we do not have any production of mass inside the tank. The total mass can be obtained by integrate $Au(x,t)$ (where A is the (constant) cross-sectional area) over an interval (x_1, x_2). Denote the total flux $\Phi(u, \frac{\partial u}{\partial x})$ and put $\Phi(u, \frac{\partial u}{\partial x}) = F(u) - d_{\text{comp}}(u)\frac{\partial u}{\partial x}$. This can be done since $\gamma(x) = 1$ in the considered region. Also notice that both F and d_{comp} only depend on the concentration u. From

this, the conservation law can be written as [3]

$$\frac{d}{dt}\int_{x_1}^{x_2} Au(x,t)dx = A(\Phi|_{x_1} - \Phi|_{x_2}). \tag{26}$$

The model requires that we have an expression for Φ. One choice is to use the relation

$$F(u) = uv_{\text{hs}}(u), \tag{27}$$

where $v_{\text{hs}} = v_0 \text{e}^{-r_V u}$, v_0 is the velocity of a particle that does not interfere with any other particle and r_V is a parameter. In order to get an expression for Φ, we also need the compression function $d_{\text{comp}}(u)$. According to [3] this can be written

$$d_{\text{comp}}(u) = \frac{\rho_{\text{s}}}{(\rho_{\text{s}} - \rho_{\text{f}})g} v_{\text{hs}}(u)\sigma_{\text{e}}'(u). \tag{28}$$

Here ρ_{s} and ρ_{f} are the solid and fluid densities respectively, g the acceleration of gravity and one simple choice of $\sigma_{\text{e}}(u)$ is

$$\sigma_{\text{e}}(u) = \begin{cases} 0, & \text{if } u < u_{\text{c}} \\ a(u - u_{\text{c}}), & \text{if } u \geq u_{\text{c}}. \end{cases} \tag{29}$$

Combination of Equation (28) and Equation (29) then gives

$$d_{\text{comp}}(u) = \begin{cases} 0, & \text{if } u < u_{\text{c}} \\ \frac{\rho_{\text{s}}}{(\rho_{\text{s}} - \rho_{\text{f}})g} a v_0 \text{e}^{-r_V u}, & \text{if } u \geq u_{\text{c}}. \end{cases} \tag{30}$$

Equations (26),(27) and (30) make it possible to discretize the problem. The next section will show how to do this.

4.2 Discretization

In order to describe the discretization procedure, it is necessary to have a clear picture of the sedimentation tank. Figure 13 and 14 show two different cases. Figure 13 describes continuous sedimentation and Figure 14 batch sedimentation. From now on we will only consider batch sedimentation.

Now, divide the tank into N internal layers, see Figure 15. Every layer has the thickness $\Delta x = B/N$ and the value u_j is the average of the exact solution over the layer j, thus

$$u_j = \frac{1}{\Delta x}\int_{x_{j-1}}^{x_j} u(x,t)dx \tag{31}$$

We also know that the total flux must be zero at the top and the bottom of the tank. The boundary points have the positions $x_j = j\Delta x$ for $j = 0, ..., N$. For batch sedimentation we have $Q_{\text{f}} = 0$, $Q_{\text{uf}} = 0$, $Q_{\text{e}} = 0$ and $d_{\text{disp}} = 0$. According to Section 4.1 the conservation law can be written $\Phi(u, \frac{\partial u}{\partial x}) = F(u) - d_{\text{comp}}(u)\frac{\partial u}{\partial x}$. Then put

$$D(u) = \int_{u_{\text{c}}}^{u} d_{\text{comp}}(w)\text{d}w, \tag{32}$$

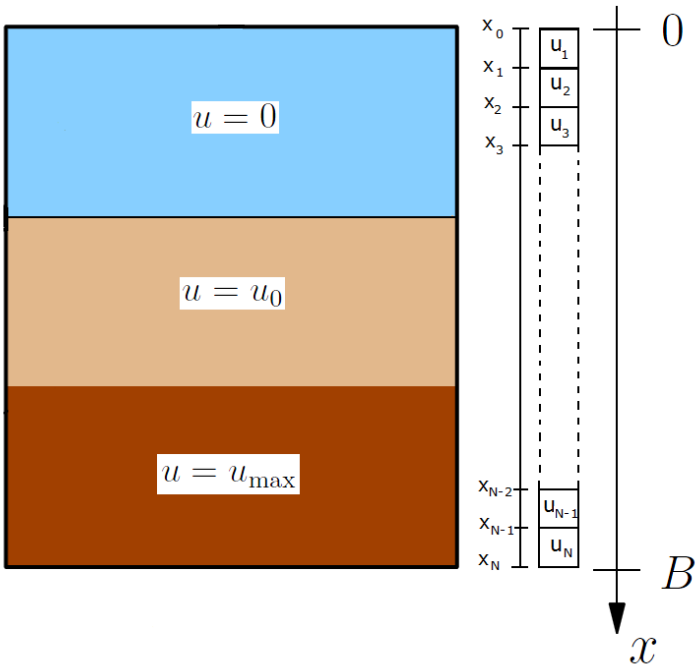

Figure 15: Discretization of the tank.

and take the derivative of D with respect to x we get

$$\frac{\partial}{\partial x} D(u) = d_{\text{comp}}(u) \frac{\partial u}{\partial x}. \tag{33}$$

Write the conservation law as

$$\Phi(u, \frac{\partial u}{\partial x}) = F(u) - J_{\text{comp}}. \tag{34}$$

By using Equation (26) and (31), we find

$$\frac{\mathrm{d}u_j}{\mathrm{d}t} = -\frac{F(u(x_j,t)) - F(u(x_{j-1},t))}{\Delta x} + \frac{J_{\text{comp}}(x_j,t) - J_{\text{comp}}(x_{j-1},t)}{\Delta x} \tag{35}$$

where we have used Equation (34) and $J_{\text{comp}}(x,t) = \gamma(x)\frac{\partial D(u)}{\partial x}$. We also need to approximate the convective flux function $F(u)$ at the boundaries between the layers. This can be done in many different ways. If the function $F(u)$ has one unique maximum point, a smart choice of approximation is the Godunov numerical flux, which reads [3]

$$G_j = G_j(u_j, u_{j+1}) = \begin{cases} \min\limits_{u_j \le u \le u_{j+1}} F(u) & \text{if } u_j \le u_{j+1} \\ \max\limits_{u_j \ge u \ge u_{j+1}} F(u) & \text{if } u_j > u_{j+1} \end{cases} \tag{36}$$

To get a complete spatial discretization we need to approximate $d_{\text{comp}}(u)$. Therefore denote the approximation of $d_{\text{comp}}(u)$ as follows:

$$J_{\text{comp}}(x_j,t) \approx \gamma(x_j) \frac{D_{j+1}^{\text{num}} - D_j^{\text{num}}}{\Delta x} \tag{37}$$

D_j^{num} can be found by Equation (32). With our choice of the function $d_{\text{comp}}(u)$ this can be done analytically.

It now remains to discretize the time. The method described above is of first order convergence in space, so we are going to use an explicit Euler scheme to discretize the time. Let u_j^n denote the concentration over layer j at time t_n, where $t_n = n\Delta t$. Use the explicit Euler step and get

$$\frac{\mathrm{d}u_j}{\mathrm{d}t}(t_n) \approx \frac{u_j^{n+1} - u_j^n}{\Delta t} \tag{38}$$

Plug this expression into Equation (35), rearrange and get:

$$u_j^{n+1} = u_j^n - \frac{\Delta t}{\Delta x}(F_j^{\text{num},n} - F_{j-1}^{\text{num},n}) + \frac{\Delta t}{\Delta x}(J_j^{\text{num},n} - J_{j-1}^{\text{num},n}) \tag{39}$$

Equation (39) shall be valid for $j = 1, ..., N$ and it is the final discretization of the batch sedimentation PDE.

It is important to note that there is a restriction on Δt to keep the scheme stable. The CFL-condition must be satisfied, which is

$$\Delta t \leq \left(\frac{1}{\Delta x} \max_{0 \leq u \leq u_{\max}} |F'(u)| + \frac{2}{\Delta x^2} \max_{0 \leq u \leq u_{\max}} d_{\text{comp}}(u) \right)^{-1}. \tag{40}$$

Inequality (40) gives us an upper bound for the time step. Violation of (40) may imply numerical instability, which means that the numerical scheme would not converge to the physically relevant solution.

4.3 Numerical solution for batch sedimentation PDE

In order to solve the batch sedimentation PDE we are going to use the numerical method described in Chapter 4.2 and implement this in MATLAB. In this program it is easy to change the parameters to see the impact they have on the final solution. Consider the following examples.

Example 1

The solution to this example is found in Figures 16 and 17. The following parameter values have been used: $v_0 = 9.75$ m/h, $r_V = 0.37$ m^3/kg, $\rho_s = 1050$ kg/m^3, $\rho_f = 998$ kg/m^3, $g = 9.81$ m/s^2, $u_{\text{c}} = 7$ kg/m^3 and $a = 2$ m^2/s^2. The convective flux function F and the function that models the compression d_{comp} are chosen according to Equation (27) and Equation (30) respectively. The initial concentration is $u_0 = 6.12$ kg/m^3 and the simulation lasts for 5 hours. The spatial domain interval is discretized into 70 cells. We see that the solution tends to a value between $u = 12$ and $u = 13$ in the bottom of the tank as the time passes. Interesting is also the the critical concentration where the compression effects are present. In this case $u_{\text{c}} = 7$ as clearly can be seen in Figure 16. The border between the clear liquid and the activated sludge is somewhere around $x = 1.4$ when 5 hours have passed. The CFL condition (40) makes $\Delta t = 1.78$ s.

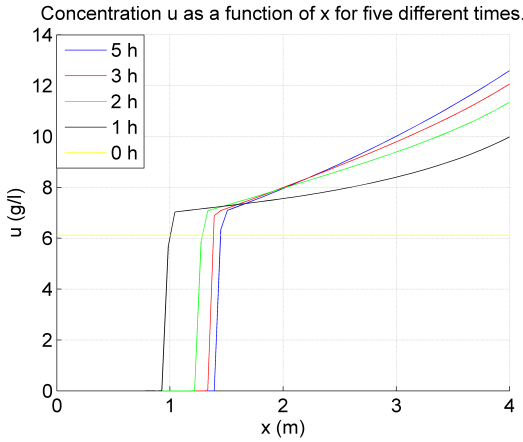

Figure 16: Solution for batch sedimentation PDE example 1, 2 dimensional plot. Parameter values: $v_0 = 9.75$, $u_c = 7$, $a = 2$, $u_0 = 6.12$, $r_V = 0.37$.

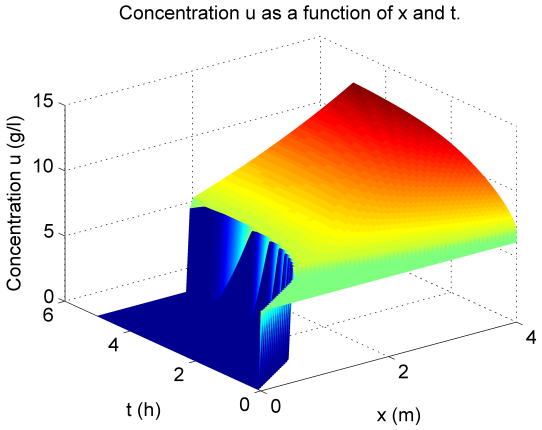

Figure 17: Solution for batch sedimentation PDE example 1, 3 dimensional plot. Parameter values: $v_0 = 9.75$, $u_c = 7$, $a = 2$, $u_0 = 6.12$, $r_V = 0.37$.

Example 2

Now we are going to investigate the impact of the parameter a. This parameter models the solid stress that the particles would be exposed to when the concentration exceeds the critical concentration u_c. This is briefly discussed in Chapter 4. A higher value of a means higher solid stress. An initial guess is that this will lead to a lower final concentration. Figures 18 and 19 show the solution. The same parameter values

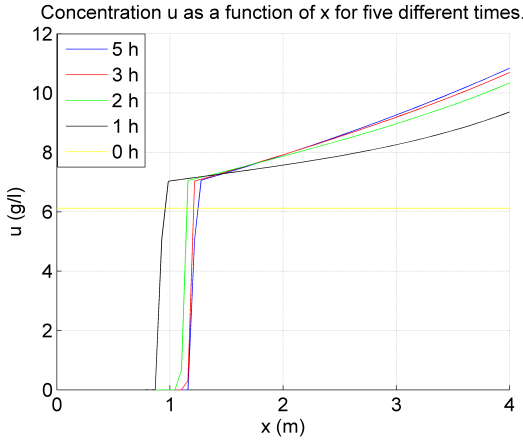

Figure 18: Parameter values: $v_0 = 9.75$, $u_c = 7$, $a = 3$, $u_0 = 6.12$, $r_V = 0.37$.

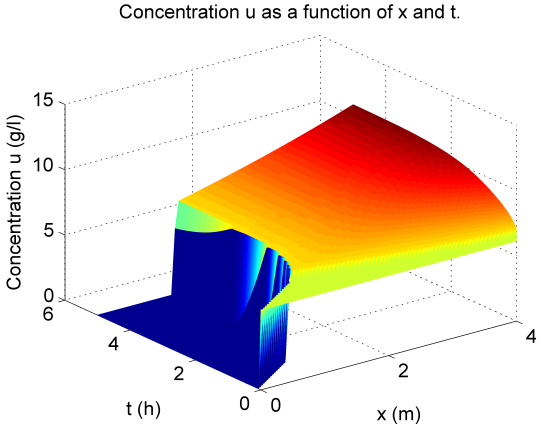

Figure 19: Parameter values: $v_0 = 9.75$, $u_c = 7$, $a = 3$, $u_0 = 6.12$, $r_V = 0.37$.

have been used as in example 1, except that we now have $a = 3$. The simulation last also for 5 hours. From Figure 18 we now see that the concentration in the bottom of the tank tends to a value around $u = 11$ kg/m^3 in the stationary state. The border between the clear liquid and the sludge is now higher up in the tank compared to situation in example 1. Now this border is around $x = 1.15$ m when $t = 5$. Also the slope of the solution from the point where $u > u_c$ and to the stationary point is more flat. The CFL condition implies $\Delta t = 1.22$ s.

Example 3

This example will discuss what happens when the initial concentration changes. Here we have the same parameters as in example 1, except that $u_0 = 4$. Figures 20 and 21 show the solution. Not very surprisingly the stationary concentration is now lower compared to example 1. Also the border between clear liquid and sludge is significantly lower, approximately $x = 2$. Notice also that there is hardly any difference between the concentration profile after 3 hours and 5 hours. The CFL condition is independent of u_0, thus $\Delta t = 1.78$ s as in example 1.

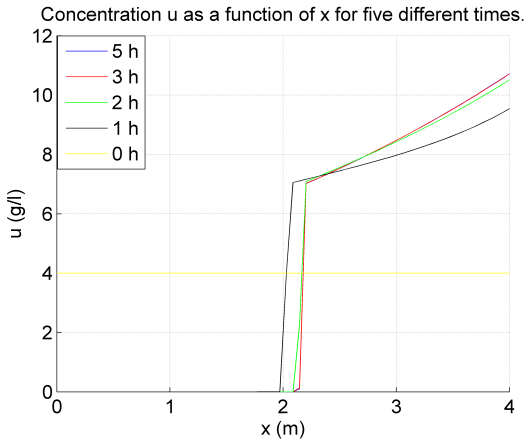

Figure 20: Parameter values: $v_0 = 9.75$, $u_c = 7$, $a = 2$, $u_0 = 4$, $r_V = 0.37$.

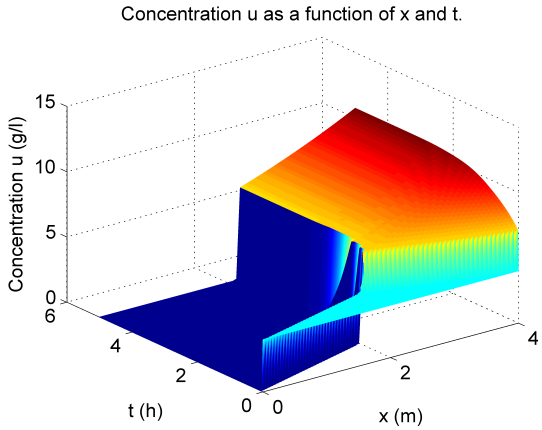

Figure 21: Parameter values: $v_0 = 9.75$, $u_c = 7$, $a = 2$, $u_0 = 4$, $r_V = 0.37$.

Example 4

The next parameter to investigate is u_c. Put $u_c = 9$ and keep all other parameters constant as in example 1. Figure 22 and 23 show what is happening. In the bottom the concentration is around $u = 14$ when $t = 5$ and the border between clear liquid and sludge is lower, now approximately at the point $x = 1.8$. The CFL is now $\Delta t = 3.42$ s.

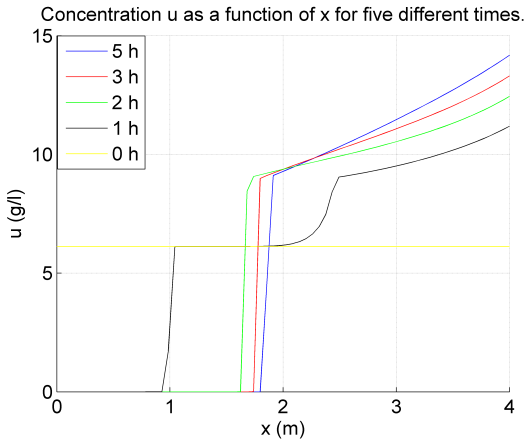

Figure 22: Parameter values: $v_0 = 9.75$, $u_c = 9$, $a = 2$, $u_0 = 6.12$, $r_V = 0.37$.

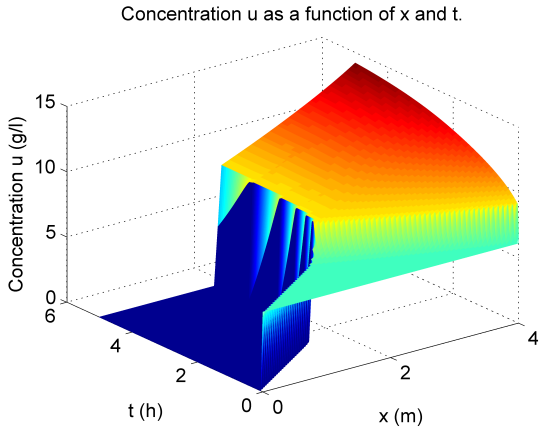

Figure 23: Parameter values: $v_0 = 9.75$, $u_c = 9$, $a = 2$, $u_0 = 6.12$, $r_V = 0.37$.

Example 5

Now keep all constants in example 1 unchanged, but put $v_0 = 15$. The result is shown in Figure 24 and 25. Here we see that this case is not profoundly different from the case in example 1. However, two small differences can be found. For small times the border between clear liquid and sludge is slightly lower in the tank. Also, the concentration is higher in the bottom of the tank for small times. The CFL condition: $\Delta t = 1.16$ s.

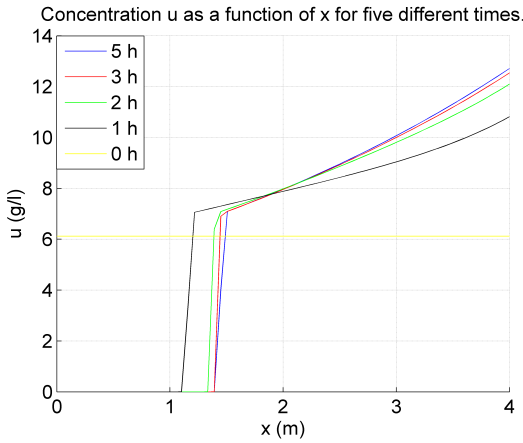

Figure 24: Parameter values: $v_0 = 15$, $u_c = 9$, $a = 2$, $u_0 = 6.12$, $r_V = 0.37$.

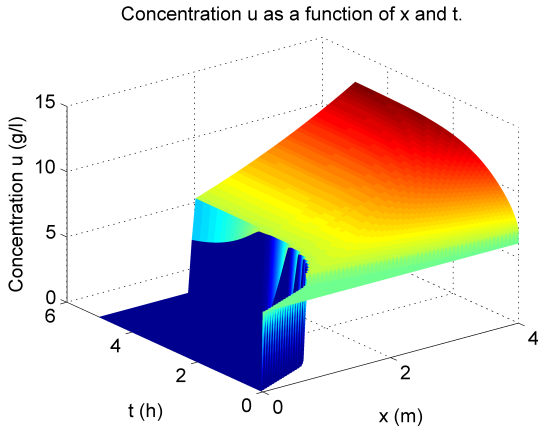

Figure 25: Parameter values: $v_0 = 15$, $u_c = 9$, $a = 2$, $u_0 = 6.12$, $r_V = 0.37$.

Example 6

This is the last example and it will discuss the impact of the parameter r_V. As usual, use the same constants as in example 1 but with $r_V = 0.2$. The solution is shown in Figure 26 and 27.

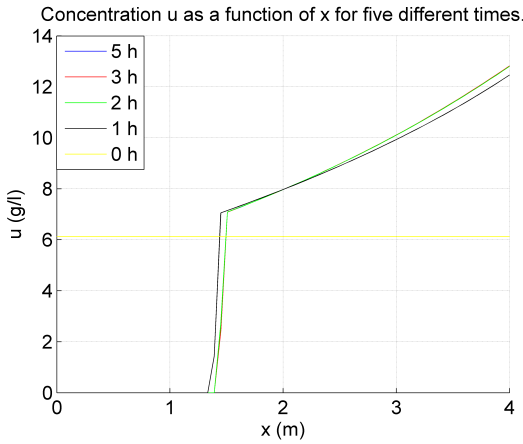

Figure 26: Parameter values: $v_0 = 9.75$, $u_c = 9$, $a = 2$, $u_0 = 6.12$, $r_V = 0.2$.

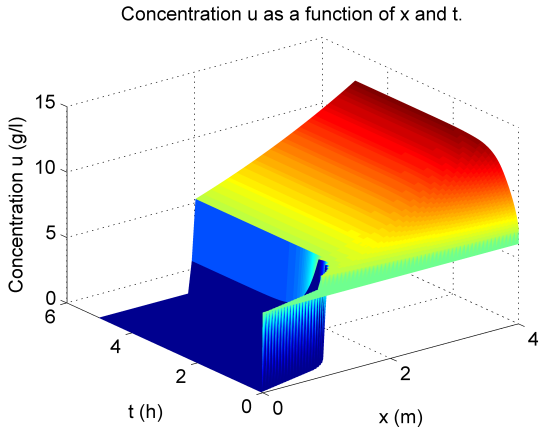

Figure 27: Parameter values: $v_0 = 9.75$, $u_c = 9$, $a = 2$, $u_0 = 6.12$, $r_V = 0.2$.

Clearly, the solution becomes stationary much faster in this case. After 2 hours there is in principle no differences between the solutions. Moreover, the CFL condi-

tion is now much lower, $\Delta t = 0.57$ s. The conclusion is that the CFL condition is very sensitive for changes in the parameter r_{V}.

5 Adjustment of parameters a and u_c to fit synthetic data

This section will discuss some properties of the parameters a and u_c and investigate the inverse problem of determining these two parameters from data by solving a minimization problem. Here we will consider synthetic data to see if the implementation is correct and that the model is able to produce a relevant solution. Therefore, suppose that we solve the batch sedimentation PDE with the parameter values $a = 3$ and $u_c = 7$. Denote this solution u. Then, add to this solution a normal distributed noise, with zero mean and a certain variance. Let us call this the *disturbed solution* and denote it by d. Now we need some measure to quantify difference between solutions. Introduce a function J according to

$$J(a, u_c) = \sum_{t_i} \sum_{x_j} (u(x_j, t_i) - d(x_j, t_i))^2 \tag{41}$$

The solution u that best approximates the disturbed solution in the least square sense is the solution we will look for. This can be formulated as an optimization problem:

$$\begin{cases} \text{minimize} & J(a, u_c) \\ \text{subject to} & a \geq 0, \quad 0 \leq u_c \leq u_{\max}. \end{cases} \tag{42}$$

Obviously, J is a function of a and u_c, so we want to find the point (a^*, u_c^*) that satisfies (42). J is quadratic, but the constraints do not define a compact set. However, for large a the function J will grow, so we can restrict the value of a, making the set defined by the constraints compact. Since J is continuous, it follows from Weierstrass theorem that a minimum exists [5].

To illustrate the minimization procedure, we will take a closer look att three different cases. The parameter values are found in Table 1.

N	70	(Number of x-steps)
u_0	3.67	(Initial concentration)
H	1	(Height of the tank in meters)
T	1	(Simulation time in hours)
v_0	3.47	
r_V	0.37	
ρ_s	1943	
$\Delta\rho$	945	
g	9.81	
u_c	7	
a	3	

Table 1: Parameter values.

5.1 Case I (small disturbance)

First we treat the case when the standard deviation of the disturbance is low, so we add zero mean, normal distributed noise with standard deviation $\sigma = 0.05$ to the solution of the PDE with the parameter values $a = 3$ and $u_c = 7$. The next step is to try to find back to the point $(a, u_c) = (3, 7)$ by solving (42), i.e. minimizing J. There are several built in routines in MATLAB for this purpose. To visualize the problem, it is also advantageous to also plot level curves for J. Figure 28 shows the level curves for J and Figure 29 the disturbed solution. Not very surprisingly the minimum is attained at the point $(a, u_c) = (3, 7)$ where $J_{\min} = 17.9763$. We see also that J grows fast as a gets larger combined with that u_c gets smaller, and vice versa. Note also the curve where J does not grow very fast. The change in one of the parameter seems to cancel out the change in the other.

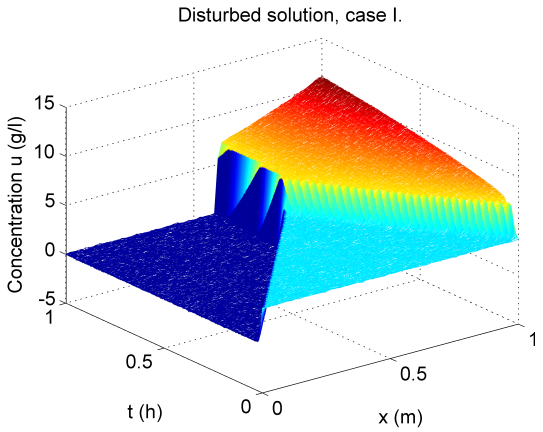

Figure 28: Disturbed solution, $\sigma = 0.05$, $J_{\min} = 17.9763$.

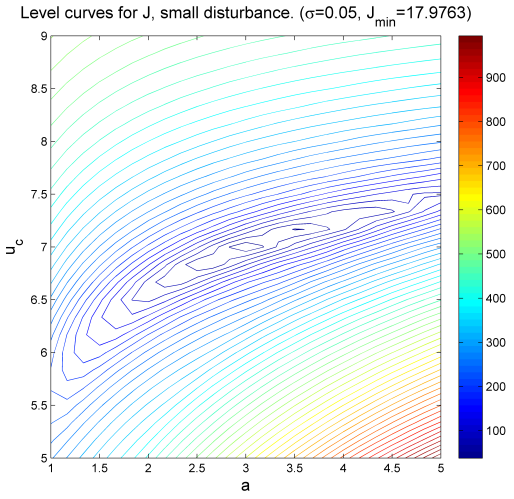

Figure 29: Level curves for J, $\sigma = 0.05$, $J_{\min} = 17.9763$.

5.2 Case II (medium disturbance)

Now increase the standard deviation to $\sigma = 0.3$. The result is shown in Figure 30 and 31. The structure of J is rather similar to that in case I, but with significantly larger minimum value, $J_{\min} = 108.2623$. It can also be observed that the function does not seem to grow as fast as in case I around the minimum point, $(a, u_c) = (3, 7)$. The level curves are more sparse there.

5.3 Case III (high disturbance)

Finally, increase the standard deviation to $\sigma = 1.5$ and obtain the result in Figure 32 and 33. The same pattern is repeated. The minimum value is larger, $J_{\min} = 540.3623$, and the level curves around the minimum point are more sparse.
In order to investigate if the numerical method is able to find the minimum point,

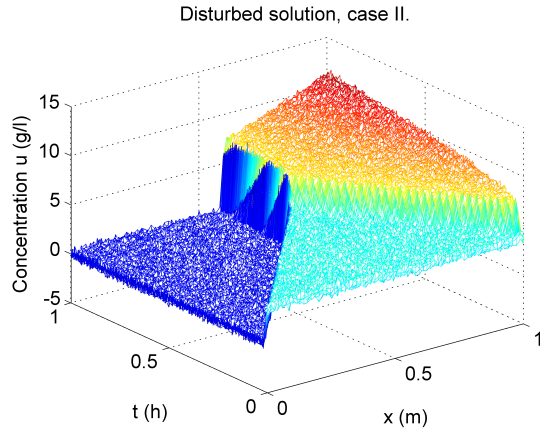

Figure 30: Disturbed solution, $\sigma = 0.3$, $J_{\min} = 108.2623$.

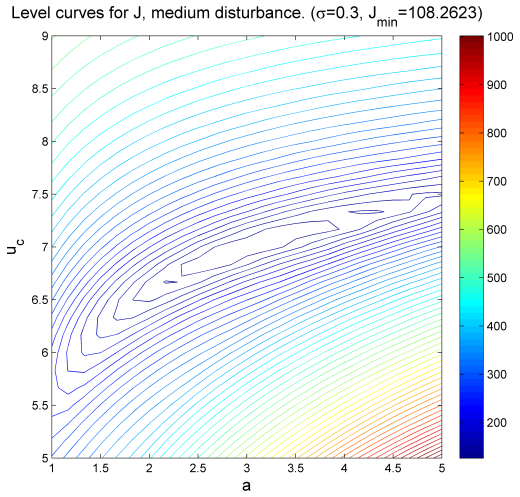

Figure 31: Level curves for J, $\sigma = 0.3$, $J_{\min} = 108.2623$.

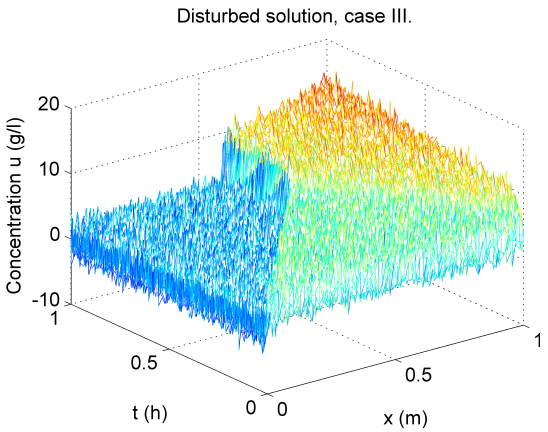

Figure 32: Disturbed solution, $\sigma = 1.5$, $J_{\min} = 540.3623$.

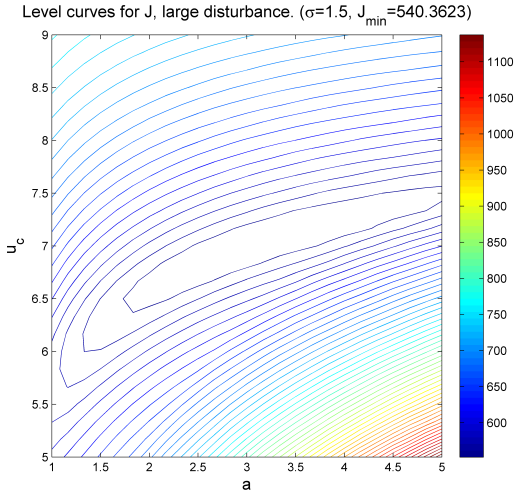

Figure 33: Level curves for J, $\sigma = 1.5$, $J_{\min} = 540.3623$.

which is $(a, u_c) = (3, 7)$ consider Figure 34. The simulation has now been going for 200 minutes. The red line shows iterations with the multidimensional search method Nelder-Mead. It takes the algorithm 26 iterations to reach the minimum point $(a, u_c) = (2.9915, 6.9953)$, when starting at the point $(a, u_c) = (5, 8)$.

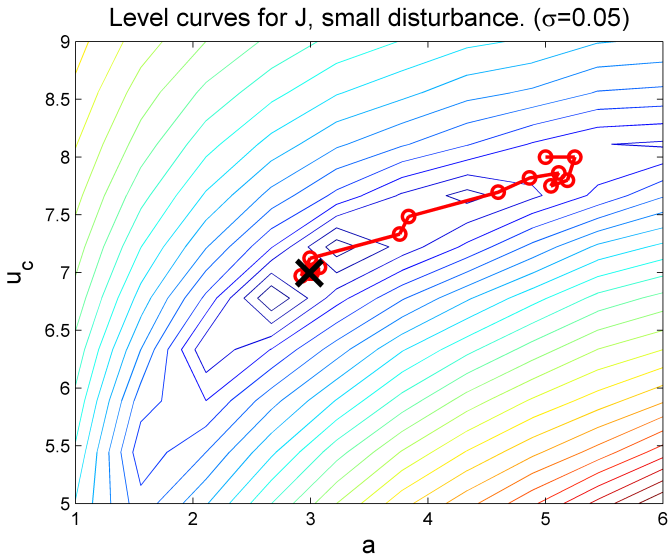

Figure 34: Level curves for J, $\sigma = 0.05$. In red, iterations with Nelder-Mead algorithm.

6 Real data and functional

As mentioned earlier, the main topic of this paper is to investigate if it is possible to find parameter values for the compression function described in Chapter 4. The available data are from a wastewater treatment plant in Deinze, Belgium. The measurement procedure is described in [2] and [1].

6.1 Illustration of measured data

Figures 35-40 show the data sets for the three different initial concentrations. As

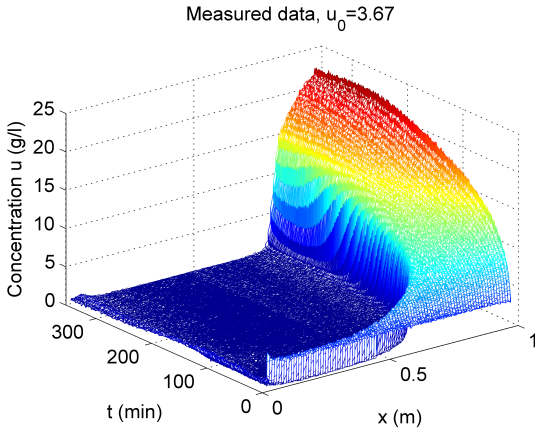

Figure 35: Measured data, $u_0 = 3.67$ g/l

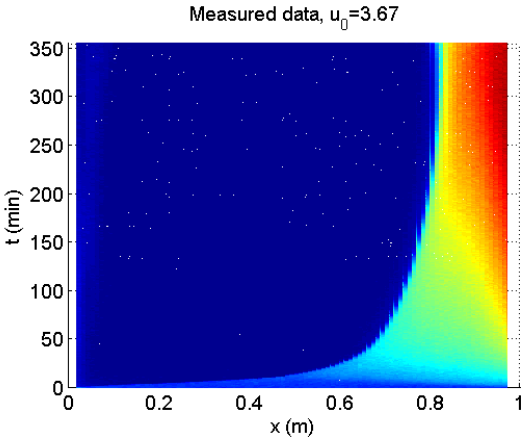

Figure 36: Measured data, $u_0 = 3.67$ g/l

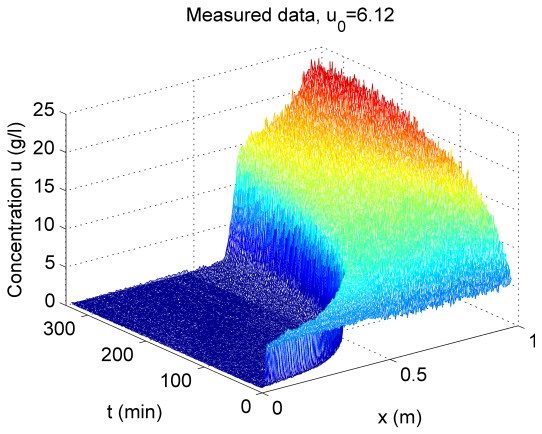

Figure 37: Measured data, $u_0 = 6.12$ g/l

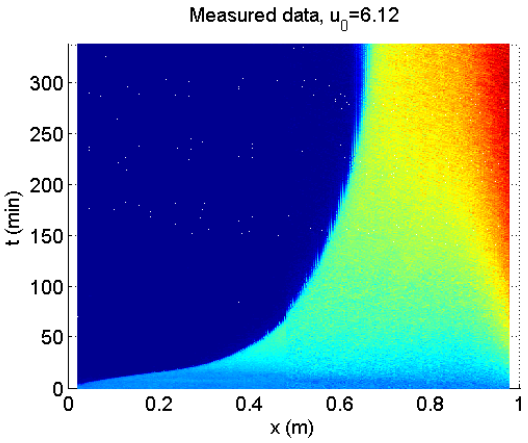

Figure 38: Measured data, $u_0 = 6.12$ g/l

can be seen from the figures, the different cases differ a lot. From the cases when $u_0 = 6.12$ g/l and $u_0 = 7.29$ there is an induction period in the initial phase, where no sedimentation takes place. This induction period highly depends on the initial concentration u_0 and it will be discussed later in this paper.

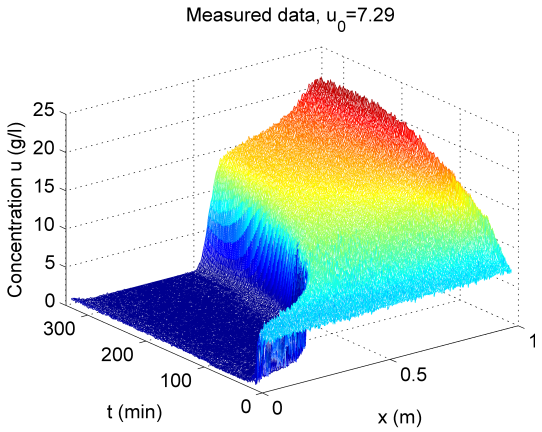

Figure 39: Measured data, $u_0 = 7.29$ g/l

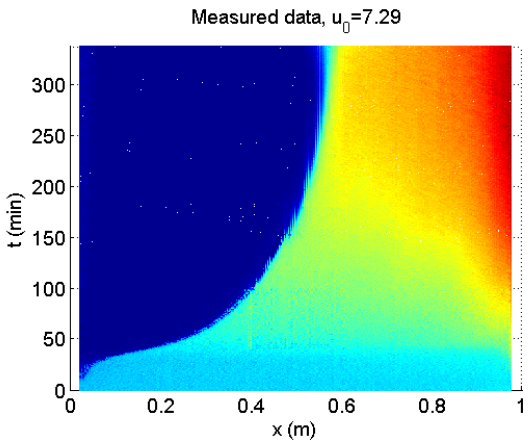

Figure 40: Measured data, $u_0 = 7.29$ g/l

6.2 Functional

In order to find the parameter values of the model, we have to measure the error between the simulation and the data. Therefore we will define a functional J in a way that it will measure the error. The task is then to minimize J.

For this purpose it is necessary to get a clear picture of the data sets. Totally three sets are available. For the case with $u_0 = 3.67$ g/l the experiment lasts for 21270 seconds and for the other two 20250 seconds. The spatial discretization is equidistant and the same for all three. The time discretization is not equidistant. All three experiment has its first value at $t_1 = 15$ s. Here we define $\Delta t_i = t_{i+1} - t_i$ where i is the index for time point i. For all three experiments it holds that

$$\Delta t_i = \begin{cases} 30 \text{ s}, & i = 1, ..., 239 \\ 45 \text{ s}, & i = 240 \\ 60 \text{ s}, & i = 241, ..., M \end{cases}$$

where M is the total number of time points. For $u_0 = 3.67$, $M = 475$ and for both $u_0 = 6.12$ and $u_0 = 7.29$, $M = 458$. By putting $\Delta t = 30$ s, Δt_i can be written

$$\Delta t_i = \begin{cases} \Delta t \ , & i = 1, ..., 239 \\ \frac{3}{2}\Delta t \ , & i = 240 \\ 2\Delta t \ , & i = 241, ..., M \end{cases}$$

In space, the total number of data points is $N = 191$. The tank is 1 meter high which means that the data points are not symmetrically placed on the x-axis. The first value is $x_1 = 0.00225$ m and the last $x_N = 0.97725$ m. The distance between the data points are $\Delta x_j = x_{j+1} - x_j = 0.0050$ m for all j. Therefore we can define Δx without index j. It is now possible to define the functional J. To be able to compare functional values from different time intervals T, in order to investigate in which time intervals the functional is largest, we need to, in some sense, normalize

the functional. We want to minimize the integral

$$J = \frac{1}{HT}\int_0^T\int_0^H (u_{\text{data}}(x,t) - u_{\text{PDE}}(x,t))^2 dxdt \tag{43}$$

where H is the height, T is the time, u_{data} is the data points and u_{PDE} is the solution to the PDE. When discretizing the functional, the integral turns into a sum:

$$J = \frac{1}{HT}\sum_i\sum_j (u_{\text{data}}(x_i,t_j) - u_{\text{PDE}}(x_i,t_j))^2 \Delta x_i \Delta t_j \tag{44}$$

Since $\Delta x_i = \Delta x$ is constant, this can be written as

$$\begin{aligned} J = \frac{\Delta x}{H^* T}\sum_i\sum_j (u_{\text{data}}(x_i,t_j) - u_{\text{PDE}}(x_i,t_j))^2 \Delta t_j = \\ \frac{1}{NT}\sum_i\sum_j (u_{\text{data}}(x_i,t_j) - u_{\text{PDE}}(x_i,t_j))^2 \Delta t_j \end{aligned} \tag{45}$$

since $H^*/\Delta x = N$, where $H^* = x_N - x_1 + \Delta x = 0.95 + 0.005 = 0.955$ m. At the time point that corresponds to $i = 240$, Δt_i goes from 30 seconds to 45 seconds. Denote this by M^*. The time point that corresponds to $i = 242$, Δt_i goes from 45 seconds to 60 seconds. Denote this time point M^{**}. The functional can then be written

$$\begin{aligned} J = \frac{1}{NT}\sum_{i=1}^{N}(\sum_{j=1}^{M^*}(u_{\text{data}}(x_i,t_j) - u_{\text{PDE}}(x_i,t_j))^2 \Delta t + \\ 3/2(u_{\text{data}}(x_{241},t_{241}) - u_{\text{PDE}}(x_{241},t_{241})\Delta t + 2\sum_{j=M^{**}}^{M}(u_{\text{data}}(x_i,t_j) - u_{\text{PDE}}(x_i,t_j))^2 \Delta t) \end{aligned} \tag{46}$$

Equation (46) can be simplified, by factorization and putting $M^* = 240$ and $M^* = 242$:

$$\begin{aligned} J = \frac{\Delta t}{NT}\sum_{i=1}^{N}(\sum_{j=1}^{240}(u_{\text{data}}(x_i,t_j) - u_{\text{PDE}}(x_i,t_j))^2 + \\ 3/2(u_{\text{data}}(x_{241},t_{241}) - u_{\text{PDE}}(x_{241},t_{241}) + 2\sum_{j=242}^{M}(u_{\text{data}}(x_i,t_j) - u_{\text{PDE}}(x_i,t_j))^2) \end{aligned} \tag{47}$$

Functional (47) makes it possible to compare a simulation with data on a time interval of arbitrary length. Functional (47) is also called L^2-norm. It is also possible to define a L^1-norm by replacing the squares in the sum by an absolute value.

6.3 Adjustment of parameters a and u_c to fit real data

In Chapter 5 we solved the minimization problem (42), i.e. we were looking for a solution u that approximated the disturbed solution. Here we are trying to do the

same thing, but with the real data and the functional defined in 6.2.

The values of v_0 and r_V are retrieved from [7]. We will here use the Vesilind hindered settling velocity function defined in Chapter 4. The problem is then to minimize $J(a, u_c)$. The strategy is to plot level curves for J in some region in the (a, u_c)-plane to get an estimate where the minimum point is located, after which we will use the Nelder-Mead-simplex algorithm to find the minimum point. The reason for plotting the level curves is that we get an overview of $J(a, u_c)$. Moreover, as seen in Figure 41 and Figure 42 some values of a and u_c have been omitted, because these values imply a very small Δt, which make the simulation slow, and also because the values for J is much larger in these regions. Totally four simulations were done, two for $u_0 = 6.12$ g/l and two for $u_0 = 3.67$ g/l. We also use the L^1-norm to see if there is large differences between if the error is measured in L^1-norm or in L^2-norm. We

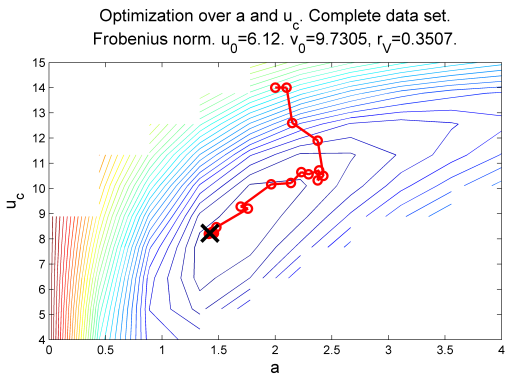

Figure 41: Level curves for J, $u_0 = 6.12$ g/l. L^2-norm. $J = 0.52$ at $(1.42, 8.22)$.

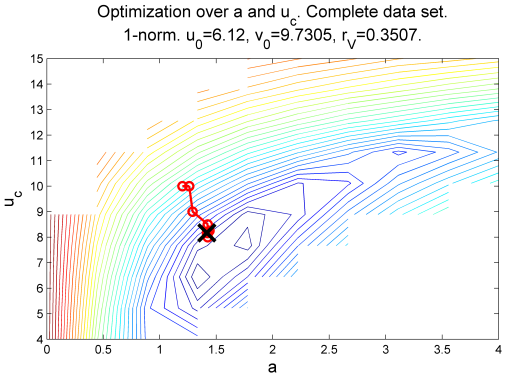

Figure 42: Level curves for J, $u_0 = 6.12$ g/l. L^1-norm $J = 57.06$ at $(1.42, 8.16)$.

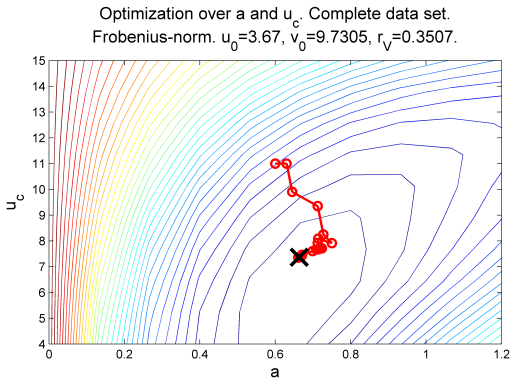

Figure 43: Level curves for J, $u_0 = 3.67$ g/l. L^2-norm. $J = 0.40$ at $(0.66, 7.36)$.

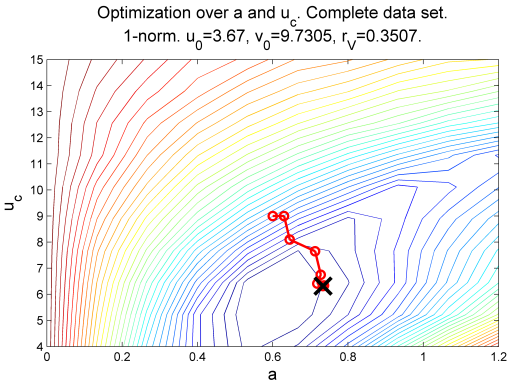

Figure 44: Level curves for J, $u_0 = 3.67$ g/l. L^1-norm. $J = 38.23$ at $(0.73, 6.32)$.

notice that both a and u_c are larger for the larger initial concentration. Now we are going to take a look at the parameters v_0 and r_V. The next section will proceed with an optimization of all the four parameters at the same time.

6.4 Optimization over a, u_c, v_0 and r_V simultaneously

The next procedure is to minimize over the four parameters a, u_c, v_0 and r_V simultaneously. Here we take the points found in the previous section as the initial point in the Nelder-Mead algorithm. Table 2 summarizes the different cases, where the point is (r_V, v_0, u_c, a). In order to see how well the model describes batch sedimentation,

u_0	Final point	$J_{\min}$	Norm
6.12	$(0.46, 11.58, 6.48, 0.37)$	29.40	L^1-norm
6.12	$(0.40, 4.58, 20.20, 0.70)$	0.31	L^2-norm
3.67	$(0.46, 11.75, 4.37, 0.30)$	23.72	L^1-norm
3.67	$(0.45, 7.66, 0.006, 0.11)$	0.23	L^2-norm

Table 2: Optimization over r_V, v_0, u_c and a.

form the difference between the model with the parameters given by Table 2 and the measured data. Figures 45 - 52 show the results. Obviously, the result is better than in the previous section, but still not satisfactory. The model has big problem

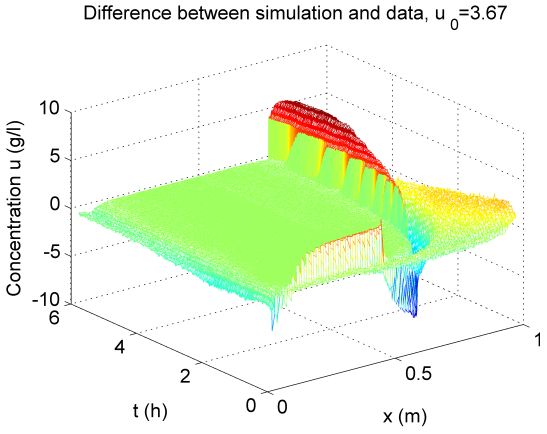

Figure 45: Difference between simulation and data, $u_0 = 3.67$ g/l, L^1-norm.

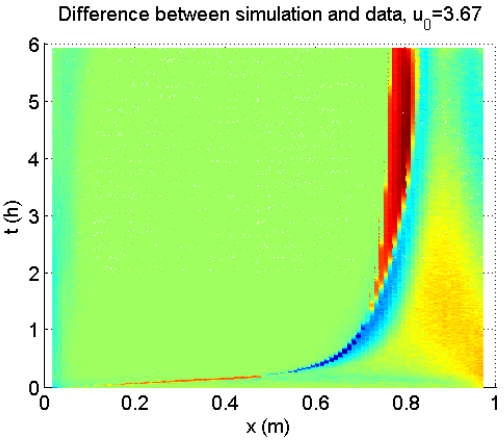

Figure 46: Difference between simulation and data, $u_0 = 3.67$ g/l, L^1-norm.

with the first 2 hours. It seems that the concentration is way too high in the bottom of the tank for small times. Here we have not treated the induction period at all. Therefore the solution is way of initially. It is also worth noticing that the L^2-norm produces a better solution around the shock wave. However, the induction period is a problem that we will try to solve in the next section.

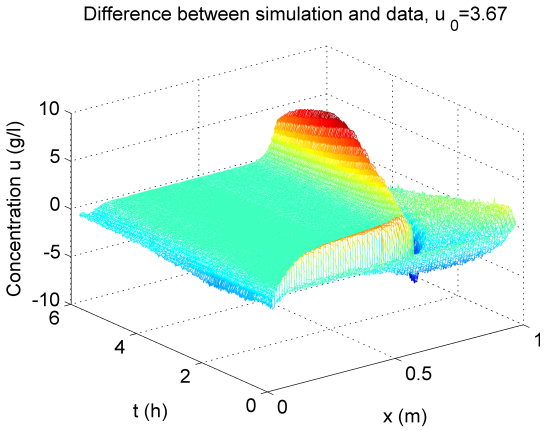

Figure 47: Difference between simulation and data, $u_0 = 3.67$ g/l, L^2-norm.

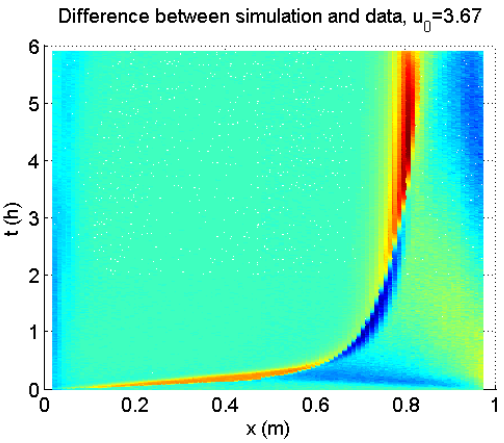

Figure 48: Difference between simulation and data, $u_0 = 3.67$ g/l, L^2-norm.

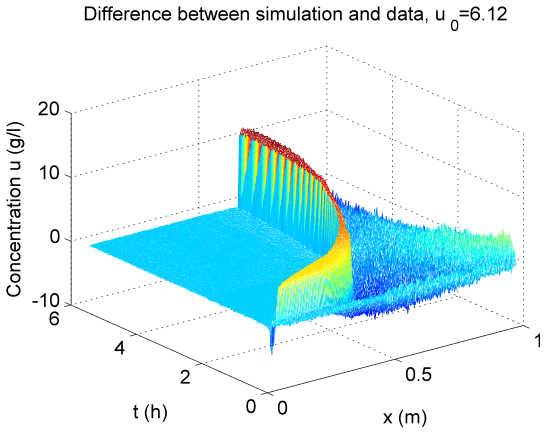

Figure 49: Difference between simulation and data, $u_0 = 6.12$ g/l, L^1-norm.

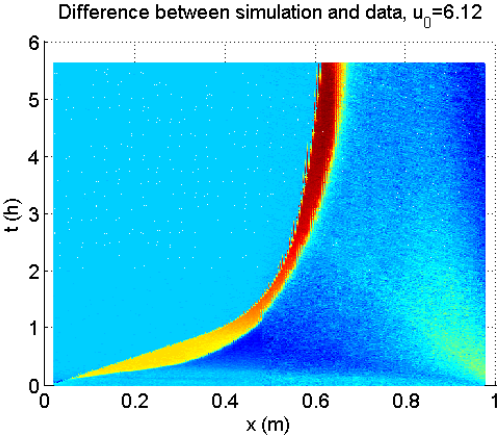

Figure 50: Difference between simulation and data, $u_0 = 6.12$ g/l, L^1-norm.

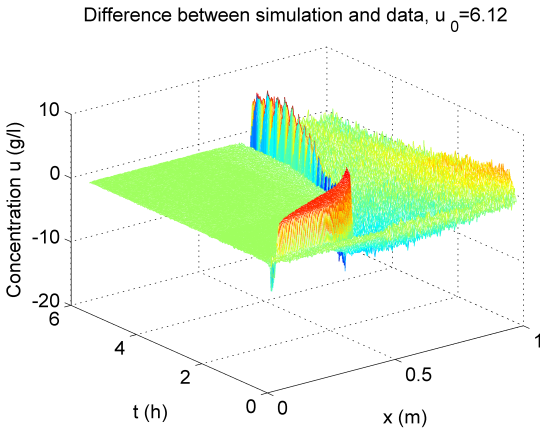

Figure 51: Difference between simulation and data, $u_0 = 6.12$ g/l, L^2-norm.

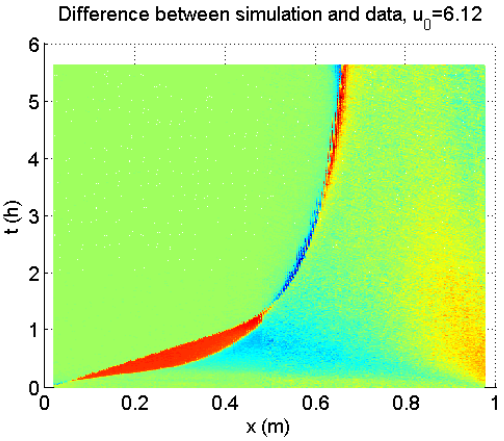

Figure 52: Difference between simulation and data, $u_0 = 3.67$ g/l, L^2-norm.

7 Graphical approach to model induction period

This section will deal with the induction period. For small times, an induction period can be observed i.e. a time period in the initial phase where no sedimentation is present first and then gradually the settling velocity increases. This induction period is longer for higher initial concentrations and can be neglected for the case $u_0 = 3.67$ g/l. We assume that the equation for the upper particle reads

$$x'(t) = g(t)v_{\text{hs}}(u_0) \tag{48}$$

where $g(t)$ is a function increasing from 0 and 1, defining the induction period and $v_{\text{hs}}(u_0)$ is the hindered settling velocity at concentration u_0. Put $K = v_{\text{hs}}(u_0)$, integrate from 0 to t and get:

$$x(t) - x(0) = \int_0^t g(\xi)Kd\xi = K\int_0^t g(\xi)d\xi \tag{49}$$

or

$$x(t) = x(0) + \int_0^t g(\xi)Kd\xi = x(0) + K\int_0^t g(\xi)d\xi \tag{50}$$

The values for $K = v_{\text{hs}}(u_0)$ can be found in the following way. Define

$$m(x,t) = \int_0^x u(\xi,t)d\xi \tag{51}$$

Then $m(x,t)$ is the mass per area unit between 0 and x at time t. Figures 53-55 show the level curves for the function $m(x,t)$. They can be interpreted as isomass curves. The particles form a queue, like cars in a traffic flow, where no car overtakes another.
Since we know that $0 \leq g(t) \leq 1$, it follows that $v_{\text{hs}}(u_0)$ is obtained where $x'(t)$ has

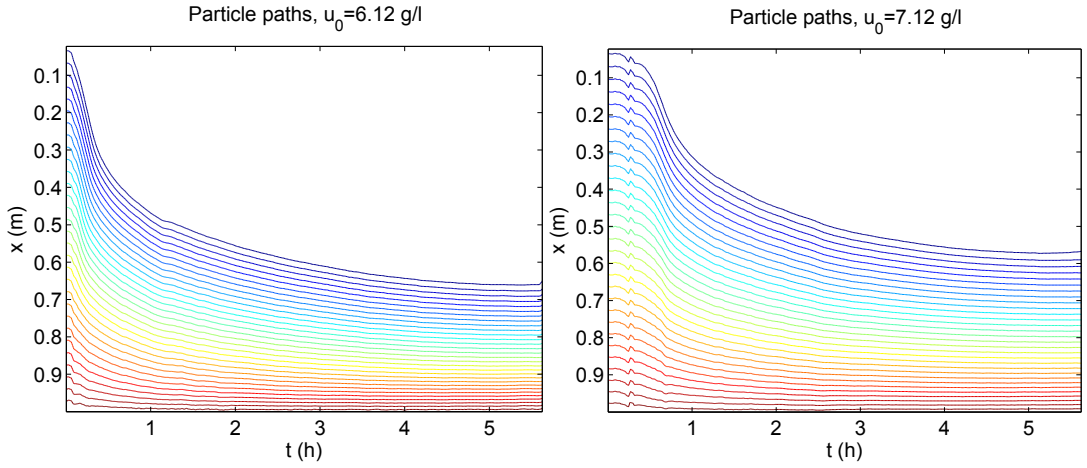

Figure 53: Level curves for $m(x,t)$, $u_0 = 6.12$ g/l.

Figure 54: Level curves for $m(x,t)$, $u_0 = 7.29$ g/l.

its maximum. By differentiation the data, we find the maximum points in Figures 56-58. Due to noise it is not easy to see the maximum for $u_0 = 3.67$. The reason for

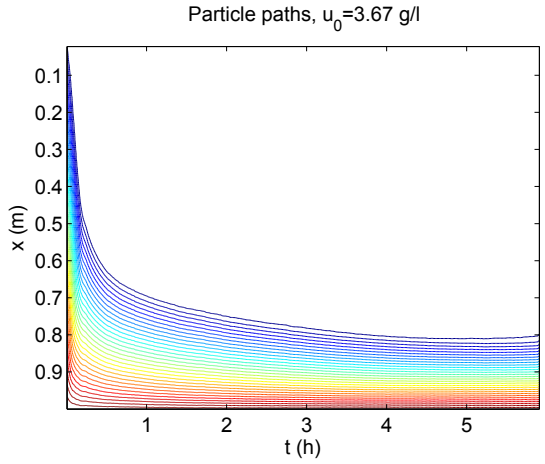

Figure 55: Level curves for $m(x,t)$, $u_0 = 3.67$ g/l.

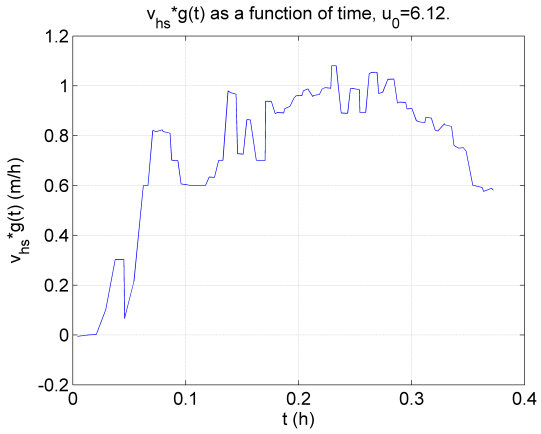

Figure 56: $g(t)v_{\rm hs}$ as a function of time, $u_0 = 6.12$ g/l.

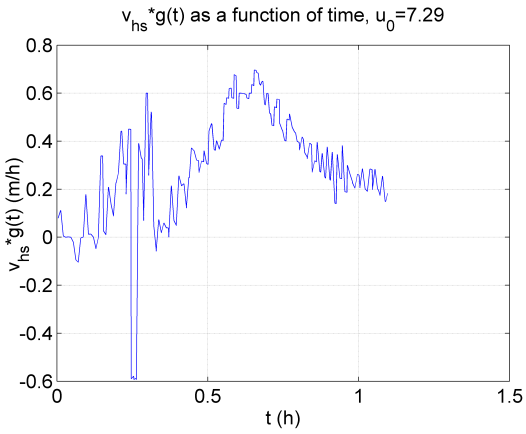

Figure 57: $g(t)v_{\rm hs}$ as a function of time, $u_0 = 7.29$ g/l.

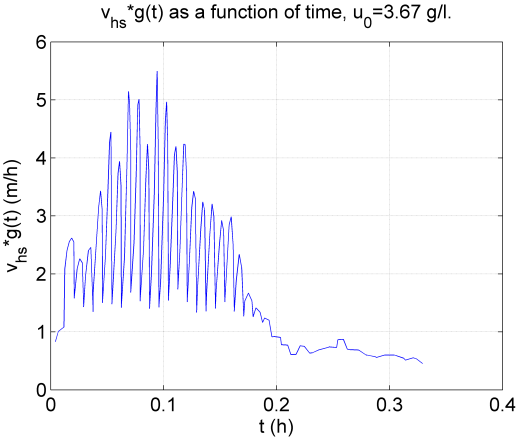

Figure 58: $g(t)v_{\rm hs}$ as a function of time, $u_0 = 3.67$ g/l.

plotting these curves is that it makes it possible to estimate the Vesilind parameters v_0 and $r_{\rm V}$. For Vesilind hindered settling velocity we have $v_{\rm hs}(u) = v_0 {\rm e}^{-r_{\rm V} u}$. Using a least square fit of the three points, gives $v_0 = 20.46$ m/h and $r_{\rm V} = 0.48$ l/g. These values have also been found by [2]. In order to find the parameters in the function $g(t)$, we want to minimize the functional

$$J(T,p) = \sum_{i=1}^{i^*} (x(t_i) + x(0) - K \int_0^{t_i} g(\xi;T,p) d\xi)^2 \tag{52}$$

where i^* is the time point that corresponds to the times where maximum in Figures 56-58 obtains and T and p are parameters in the function $g(t)$. The ansatz for $g(t)$ reads $g(\xi;T,p) = 1 - {\rm e}^{-(t/T)^p}$. Put this function $g(t)$ into the functional and obtain:

$$J(T,p) = \sum_{i=1}^{i^*} (x(t_i) + x(0) - K \int_0^{t_i} (1 - {\rm e}^{-(\xi/T)^p}) d\xi)^2 \tag{53}$$

When minimizing the functional in Equation (53) (using non linear least square) we find the result in Table 3. The result is plotted in Figures 59 and 60.

u_0 (g/l)	T (s)	p
6.12	360	1.42
7.29	1944	2.34

Table 3: Optimization over T and p.

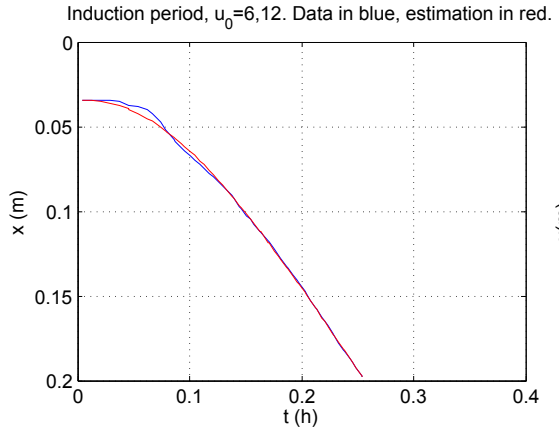

Figure 59: x (particle path) as a function of time, u_0=6.12.

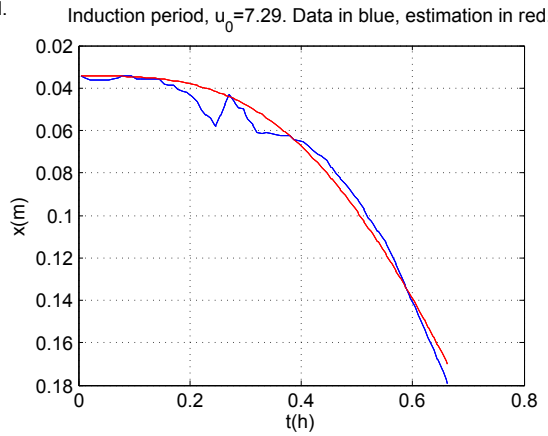

Figure 60: x (particle path) as a function of time, u_0=7.29.

8 Graphical approach to find a and u_c

8.1 Find a and u_c from steady-state profile

A similar procedure can be done in order to find the parameter values connected to the solid stress function $\sigma_e(u)$. In steady state, it holds that $u_t = 0$. The conservation law implies

$$u_t + (uv_{\text{hs}}(u) - d_{\text{comp}}(u)u_x)_x = 0 \tag{54}$$

and thus

$$uv_{\text{hs}}(u) = d_{\text{comp}}(u)u_x \tag{55}$$

Using Equation (28) then gives

$$u(x) = \frac{\rho_s}{g\Delta\rho}\sigma_e'(u)u_x(x) \tag{56}$$

Put $C = \rho_s/(g\Delta\rho)$ and observe that the right hand side of Equation (56) can be written $C\frac{\mathrm{d}}{\mathrm{d}x}\sigma_e$, giving

$$\frac{\mathrm{d}}{\mathrm{d}x}\sigma_e(u) = \frac{u(x)}{C} \tag{57}$$

Integration of Equation (57) from 0 to x then gives

$$\sigma_e(u(x)) - \sigma_e(u(0)) = 1/C\int_0^x u(\xi)d\xi \tag{58}$$

By letting $\sigma_e(u(0)) = 0$ and replace the integral by a finite sum, we get

$$\sigma_e(u) = 1/C\sum_{i=1}^{i^*} u(x_i)\Delta x \tag{59}$$

The numerical integration of Equation (59) is performed for the three initial concentrations respectively and the result is shown in Figures 61-63. The same result is found by [2]. Clearly, there are some effective solid stress present even for small concentrations. At concentrations around 13-15 g/l (which may be interpreted as the parameter u_c) a dramatic increase in effective solid stress can be observed. Note that only the last time point is used in this analysis. According to [2] it seems that the parameter u_c is time dependent. It is getting smaller for smaller times.

8.2 Find parameter values using induction period and dispersion

The values of v_0 and r_{V} found in Section 6.4 differ very much from those found in Section 7. If the parameter values found in Section 6.4 are used in the optimization in Section 7, this will lead to other values of the parameters T and p. They seem to cancel out each other. When trying to optimize over the parameter a, we can also conclude that the result is highly dependent on the initial value of the parameter in the optimization algorithm. This suggests that the problem is ill-conditioned. This

motivates us to pick out the parameter values by hand. Now, introduce a new term to the diffusion, due to dispersion

$$d_{\text{disp}}(t) = d_0 \mathrm{e}^{-t/\tau} \tag{60}$$

where d_0 and τ are parameters. By trial and error it is possible to choose values of the parameters d_0, τ, T and p in such a way that the shock-wave can be described in all three experiments with the *same* values of v_0 and r_{V}. Here only T depends on u_0, whereas the other parameters are constant. See Table 4 for parameter values and Figures 64-66 for the solutions. Note that the values of the functionals are lower than in previous sections. Due to computational difficulties, it is hard to implement an optimization algorithm to this problem, even though it is the correct scientific way to do it. However, this analysis suggests that an extra term of type (60) may be necessary in order to fully solve the problem. Constant parameters: $d_0 = 5 * 10^{-5}$ m^2/s, $v_0 = 2.65 * 10^{-3}$ m/s, $r_{\text{V}} = 0.43$ g/l, $\tau = 1000$ s, $p = 4$. No compression is considered.

u_0 (g/l)	T (s)	J
3.67	0	0.23
6.12	215	0.29
7.29	1500	0.28

Table 4: Parameter values for induction period and corresponding functional value.

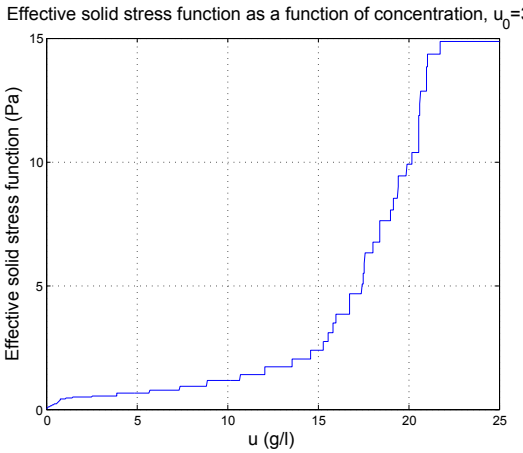

Figure 61: Effective solid stress function, u_0=3.67, steady-state.

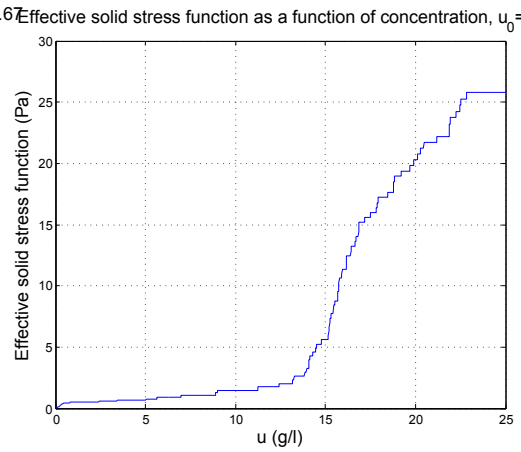

Figure 62: Effective solid stress function, u_0=6.12, steady-state.

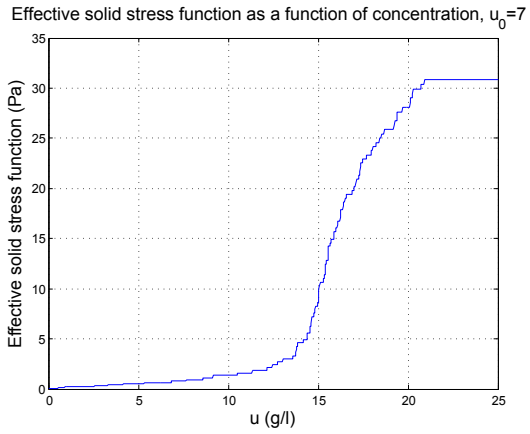

Figure 63: Effective solid stress function, u_0=7.29, steady-state.

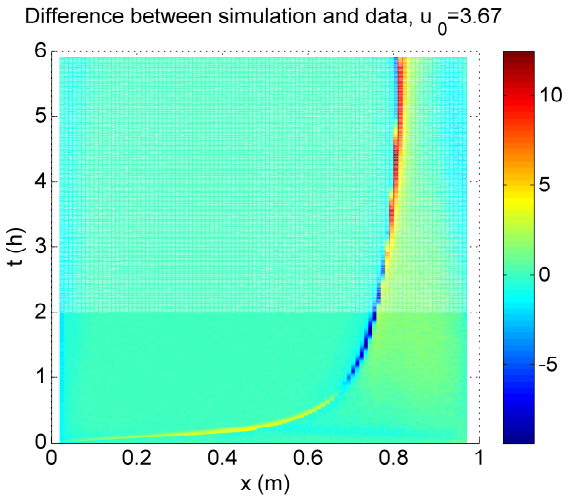

Figure 64: Solution-data, u_0=3.67 g/l.

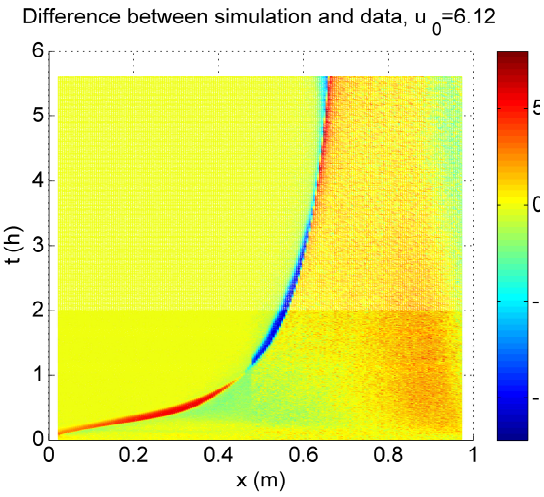

Figure 65: Solution-data, u_0=6.12 g/l.

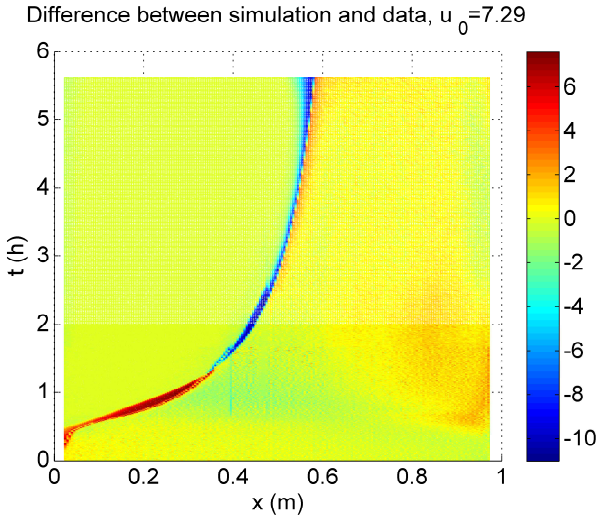

Figure 66: Solution-data, u_0=7.29 g/l.

9 Conclusion and discussion

Throughout this thesis, we have seen that the calibration problem seems hard to solve. Others have already observed the ill-posedness of the problem and this is what we also find. This can clearly be seen in the Figures in Section 6.3. The level curves for the functional J is very flat in the middle of the Figures. This means that the functional is small along a curve, which shows that the problem is ill-conditioned. Every point (a, u_c) that lies on this curve is a solution to the problem. It is also worth noticing that this will not disappear when using L^1-norm instead.

In Section 8.2 we observed that u_c were somewhere between 13 g/l and 15 g/l (for the steady-state profile) for all three experiments. But note the scale on the y-axis. The parameter a seems to depend on the initial concentration, because there are significantly higher effective solid stress for higher initial concentrations. Another problem, found by [2], is that the parameter u_c seems to depend on time. Therefore the paramater a seems to depend on u_0 in steady-state and u_c on time. It is hard to make a physical interpretation of this. If the critical concentration depends on time, it is difficult to build reliable models for continuous sedimentation.

However, we can see that by taking the induction period into consideration and adding a dispersion term that decreases with time, it is possible to handle the shock wave for all three experiments, just by choosing the parameter values by hand. The functional value may be even lower if a complete optimization over the parameters is performed.

From above it is obvious that further research in this area is needed. It is well known that many inverse problems are ill-conditioned and ill-posed. A possible way to get rid of this maybe is to collect more data or perhaps try another model structure with fewer parameters to calibrate.

References

[1] Jeriffa De Clercq, Filip Jacobs, David J. Kinnear, Ingmar Nopens, Rudi A. Dierckx, Jacques Defrancq, Peter A. Vanrolleghem: *Detailed spatio-temporal solids concentration profiling during batch settling of activated sludge using a radiotracer*. Water Research 39, 2125-2135, (2005).

[2] Jeriffa De Clercq, Ingmar Nopens, Jacques Defrancq, Ingmar Nopens, Peter A. Vanrolleghem: *Extending and calibrating a mechanistic hindered and compression settling model for activated sludge using in-depth batch experiments*. Water Research 42, 781-791, (2008).

[3] Raimund Bürger, Stefan Diehl, Sebastian Farås, Ingmar Nopens, Elena Torfs: *A consistent modelling methodology for secondary settling tanks: A reliable numerical method*. to appear in Water Science and Technology, (2013)

[4] Stefan Diehl: *Shock-Wave Behaviour of Sedimentation in Wastewater Treatment: A Rich Problem*. Springer Proceedings in Mathematics 6, (2012)

[5] Lars-Christer Böiers: *Mathematical Methods of Optimization*. Holmbergs i Malmö AB, Sweden, (2010)

[6] Stefan Diehl: *Introduction to the Scalar Non-Linear Conservation Law*. Department of Mathematics, Lund Institute of Technology, (1996)

[7] C. Fall, M. A. Espinosa-Rodriguez, N. Flores-Alamo, M. C. M. van Loosdrecht, C. M. Hooijmans: *Stepwise Calibration of the Activated Sludge Model No. 1 at a Partially Denitrifying Large Wastewater Treatment Plant*. Water Environment Research, Volume 83, Number 11, 2036-2048, (2011)

[8] R. Burger, E.M. Tory: *On upper rarefaction waves in batch settling*. Powder Technology 108, 74-87, (2000)

[9] Benjamin Seibold, Morris R. Flynn, Aslan R. Kasimov, Rodolfo Ruben Rosales: *Constructing set-valued fundamental diagrams from jamiton solutions in second order traffic models*. arXiv:1204.5510, (2012)

Master's Theses in Mathematical Sciences 2013:E36
ISSN 1404-6342

LUTFMA-3251-2013

Mathematics
Centre for Mathematical Sciences
Lund University
Box 118, SE-221 00 Lund, Sweden

http://www.maths.lth.se/